communications biology

Article

https://doi.org/10.1038/s42003-024-06996-8

Synthetic indole derivatives as an antibacterial agent inhibiting respiratory metabolism of multidrug-resistant gram-positive bacteria

Nishtha Chandal[1,2], Ritu Kalia[3], Akash Dey[3], Rushikesh Tambat[1,4], Nisha Mahey[1,2], Sanjay Jachak[3] & Hemraj Nandanwar[1,2]

The survival of modern medicine depends heavily on the effective prevention and treatment of bacterial infections, are threatened by antibacterial resistance. The increasing use of antibiotics and lack of stewardship have led to an increase in antibiotic-resistant pathogens, so the growing issue of resistance can be resolved by emphasizing chemically synthesized antibiotics. This study discovered SMJ-2, a synthetic indole derivative, is effective against all multidrug-resistant gram-positive bacteria. SMJ-2 has multiple targets of action, but the primary mechanism inhibits respiratory metabolism and membrane potential disruption. SMJ-2 was discovered to interfere with the mevalonate pathway, ultimately preventing the synthesis of farnesyl diphosphate, a precursor to the antioxidant staphyloxanthin, eventually releasing reactive oxygen species, and leading phagocytic cells to destroy pathogens. Additionally, no discernible biochemical and histopathological alterations were found in the mouse acute toxicity model. This study emphasizes mechanistic insights into SMJ-2 as a potential antibacterial with an unusual method of action.

Multidrug resistance (MDR) is one of the major causes of death globally and continues to be a significant concern in the treatment of infectious diseases[1]. *Staphylococcus aureus* is an opportunistic, commensal bacterium that colonizes about one-third of the population asymptomatically[2]. The bacteria can invade practically all organs once they break through the epithelial barrier despite the strong defenses developed by the host. The high morbidity and mortality linked to *S. aureus* infections are primarily a result of this adaptability[3]. Among the most prevalent MDR infections in the United States caused by gram-positive bacteria, include vancomycin-resistant *enterococci* (VRE), methicillin-resistant *Staphylococcus aureus* (MRSA), and *Clostridioides difficile*[4]. To increase understanding of the prevention, management, and treatment of these daunting pathogens and ameliorate patient outcomes, the Gram-Positive Committee of the Antibacterial Resistance Leadership Group was established[5].

The US Centre for Disease Control and Prevention warned in a 2019 report that we must "stop alluding to a future post-antibiotic era— because it's already here" due to the rise of antibiotic-resistant bacteria[4]. In this "post-antibiotic era," millions of people are more susceptible to infection due to surgery, cancer treatment, organ transplant, kidney dialysis, or chronic illnesses like diabetes could develop incurable diseases. It is known that MRSA is a severe bacterium that rapidly mutates when exposed to antibiotics[6]. In the past five decades (since 1980), only four new groups of antibiotics have appeared, namely streptogramins, lipopeptides (daptomycin), oxazolidinones (Linezolid), and pleuromutilins[1]. Among them, oxazolidinones were discovered by the synthetic approach[1]. Discovering novel antibiotics with fast discovery rates and minimal rates of resistance evolution is therefore necessary. Using synthetic approaches and target-based discovery may drastically alter the discovery of novel antibiotics.

This study presents two new antibacterials, SMJ-2 and SMJ-4, found fortuitously while screening for efflux pump inhibitors for the NorA efflux pump in *S. aureus*[7]. SMJ-2 and SMJ-4 did not synergize with ciprofloxacin on *norA* over-expressing *S. aureus* SA-1199B. SMJ-2 and SMJ-4 exhibit activity against all gram-positive bacteria by inhibiting various components of the TCA cycle, such as ΔpH component of transmembrane potential and

[1]Clinical Microbiology & Antimicrobial Research Laboratory, CSIR- Institute of Microbial Technology, Sector 39-A, Chandigarh, 160036, India. [2]Academy of Scientific & Innovative Research (AcSIR), Ghaziabad, Uttar Pradesh, 201002, India. [3]Department of Natural Products, National Institute of Pharmaceutical Education and Research Mohali, 160062 Mohali, India. [4]Present address: Department of Chemistry and Biochemistry, University of Oklahoma, Norman, OK, USA. e-mail: hemraj@imtech.res.in

activity of type-2 NADH dehydrogenase (NDH-2) protein by disturbing the $NADH/H^+$ pool, leading to increase in reactive oxygen species (ROS) which is a lethal to other cell types to combat infections[8]. NDH-2 has been proposed as a promising therapeutic target for human diseases since they are absent in mammals[9]. The property of this antibacterial to target these multiple components prevents pathogens from developing drug resistance in in vitro conditions. We thoroughly investigated the mechanistic underpinnings of the action of our antibacterial compound SMJ-2 on gram-positive bacteria.

Furthermore, SMJ-2 effectively eradicated pre-formed biofilms and oxacillin-induced persisters. SMJ-2 was efficacious in the mouse thigh infection model and practical enough to survive 90% of the population in the mouse peritonitis model. The in vivo acute toxicity studies demonstrate the safety of SMJ-2.

Results

Identification of SMJ-2 and SMJ-4 as antibacterials

This study introduces two new antibacterial agents, SMJ-2 and SMJ-4, which were serendipitously discovered during a screening process to identify efflux pump inhibitors targeting the NorA efflux pump in *S. aureus* SA-1199B[7]. These compounds exhibited potent antibacterial activity at remarkably low concentrations, even when tested on the *norA* overexpressing strain. Interestingly, SMJ-2 and SMJ-4 did not demonstrate synergistic effects with ciprofloxacin when tested on the *norA* overexpressing *S. aureus* SA-1199B strain. The findings suggest that these compounds neither function as substrates nor inhibitors for the *norA* overexpressing *S. aureus* (Supplementary Table 1). The compounds were further characterized (Supplementary Figs. 1–7, Supplementary Tables 2–5) and screened for antibacterial activity (Table 1). They were found rather significant against a wide variety of gram-positive bacteria, including multiple strains of the important deadly pathogens MRSA, MDR- *Enterococcus faecalis*, *Enterococcus faecium*, *Bacillus subtilis*, and *Streptococcus species*. It exhibits startlingly consistent minimal inhibitory concentrations (MIC) of 0.25 −2 μg mL^{-1} for SMJ-2 and 0.25 −16 μg mL^{-1} for SMJ-4. Notably, the MIC of SMJ-2 remained relatively unchanged in the presence of highly resistant organisms such as VRE, MRSA, ciprofloxacin-resistant strains, and erythromycin-resistant strains consistent with a mechanism of action distinct from these known antibiotics (Table 1). We aimed to evaluate the efficacy of SMJ-2 and SMJ-4 against gram-negative bacteria by determining their MICs on various strains, including *Escherichia coli*, *Pseudomonas aeruginosa*, and *Acinetobacter baumannii*. However, the compounds did not exhibit significant activity against these strains. This lack of efficacy may be attributed to the outer membrane of gram-negative bacteria, which is composed of lipopolysaccharides, potentially hindering the entry of the compounds. To investigate this, we performed a checkerboard synergy assay with polymyxin B, a membrane permeabilizer[10], at its sub-inhibitory concentration. The results showed that polymyxin B reduced the MICs of SMJ-2 and SMJ-4 by 16-fold (4 μg/mL) at 1/2 × MIC. Therefore, we concluded that the compounds were ineffective against gram-negative bacteria due to their inability to permeabilize the outer membrane (Supplementary Table 6).

SMJ-2 has a low frequency of resistant mutant generation in vitro

We tried to understand the mechanism of action of SMJ-2 and SMJ-4. Therefore, we attempted to develop SMJ-2 resistance for 21 days in vitro against *S. aureus* ATCC 29213 but could not find any. Hence, we presume that the probability of resistance development in in vitro conditions is low with SMJ-2 treatment. We tried our hands on MRSA *S. aureus* ATCC 43300 and *B. subtilis* MTCC 121 and found no significant increase in resistance development in vitro. Each biomimetic was subjected to serial passes at sub-inhibitory concentrations or levels below the MIC but could not develop resistance. As the standard medicine for treating gram-positive pathogens, ciprofloxacin, which was found to have a high incidence of spontaneous resistance generation rate, was used. The MIC of ciprofloxacin for *S. aureus* increased by approximately 512-fold after 21 days in *S. aureus* ATCC 29213, 256-fold after 26 days in *S. aureus* ATCC 43,300, and 64-fold after 21 days in *B. subtilis* MTCC 121. The MIC of the SMJ-2 either remained constant or showed a non-significant variation during that time. The findings show that SMJ-2 has a low frequency of resistant mutant generation in vitro across two species of gram-positive bacteria, i.e., *S. aureus* and *B. subtilis* (Fig. 1A–C). These observations showed that the compound might function via an unusual mode of action.

SMJ-2 and SMJ-4 display bactericidal activity on gram-positive bacteria

We subsequently conducted time-dependent killing experiments since SMJ-2 and SMJ-4 showed strong growth inhibitory effects against the *S. aureus* strain ATCC- MRSA 43300. We noticed bacterial cell death in the presence of SMJ-2 and SMJ-4 in rich media against an initial cell density of 10^5 colony-forming units (CFU) mL^{-1}. Compared to the culture control at the 0 h time point for log phase culture, SMJ-2 and SMJ-4 showed a reduction of 2.5 and 1.3 $\log_{10}$, respectively, after 12 h of treatment. As positive controls, vancomycin, linezolid, and oxacillin were used (Fig. 1D). The next step was determining whether SMJ-2 and SMJ-4 could cause bacterial cell death against MRSA 43300 in a metabolically repressed, stationary phase. We found that these compounds SMJ-2 and SMJ-4 showed almost similar activity in the stationary phase as in the log phase. We observed a reduction of 2.404 and 1.891 $\log_{10}$ after 12 h of treatment compared to the culture control at the 0 h time point for the stationary phase culture, respectively (Fig. 1E). To our astonishment, SMJ-2 outperformed vancomycin, linezolid, and oxacillin in activity during the stationary phase. SMJ-2 significantly outperforms the bulk of traditional antibiotics in its ability to kill bacteria resistant to different antibiotic classes. After 24 h, no visual turbidity was observed in the SMJ-2 and vancomycin- treated log phase bacteria (Fig. 1F). We conducted similar time-dependent killing experiments in logarithmic and stationary phase cells of *S. aureus* ATCC 29213. Here, we found a 1.93 $\log_{10}$ reduction by SMJ-2, a 2.38 $\log_{10}$ reduction by SMJ-4 after 12 h in the logarithmic phase, a 2 $\log_{10}$ reduction by SMJ-2, and a 2.15 $\log_{10}$ reduction by SMJ-4 after 12 h in stationary phase (Supplementary Fig. 8).

Since stationary-phase cells are known to contain substantial numbers of persisters, we further looked into SMJ-2's effectiveness against these cells. We created oxacillin-induced persisters, and a characteristic biphasic death pattern was noticed. Then, we treated them with various concentrations of SMJ-2 (5 × MIC, 10 × MIC, and 20 × MIC) to evaluate the effectiveness of SMJ-2 in eliminating oxacillin-induced *S. aureus* persister cells. The time-dependent persister killing assay revealed excellent anti-persister activity of SMJ-2, causing 1.8, 2.1, and 2.4 $\log_{10}$ reduction in the viable count at 5 × MIC, 10 × MIC, and 20 × MIC after 24 h. Linezolid was used here as a positive control and showed a 0.741 and 1.514 $\log_{10}$ reduction at 10 × MIC and 20 × MIC, respectively (Fig. 1G, H). SMJ-2 shows better activity than SMJ-4, and SMJ-2 showed consistent results on all bacterial strains (Table 1), while SMJ-4 showed variable results (In terms of MIC). Therefore, we used SMJ-2 to obtain further conclusive results where required.

SMJ-2 prevents bacterial growth by quenching the respiratory metabolism of bacteria

Observing SMJ-2's ability to destroy stationary phase bacterial cells and persister cells, we assumed it could be because SMJ-2 might target PMF. After all, bacterial cells require a continuous electrochemical transmembrane gradient to survive. The loss of the PMF would trigger the death of tolerant cells[11]. Therefore, to visualize changes in the electrochemical transmembrane gradient, we used the carbocyanine dye 3;3,3′-Diethyloxacarbocyanine Iodide [DiOC2(3)], and we discovered that SMJ-2 and SMJ-4, similar to the positive control carbonyl cyanide 3-chlorophenylhydrazone (CCCP) resulted in a change in membrane potential (Supplementary Fig. 9A). CCCP shows complete killing of *S. aureus* ATCC 43,300 at 10 × MIC, while SMJ-2 and SMJ-4 led a reduction of 2.5 and 1.3 $\log_{10}$ after 12 h of treatment (Supplementary Fig. 9B). There are two components of membrane potential $\Delta\Psi$ and ΔpH; now, to further examine SMJ-2 and

Table 1 | MIC values of SMJ-2 and SMJ-4 against various strains

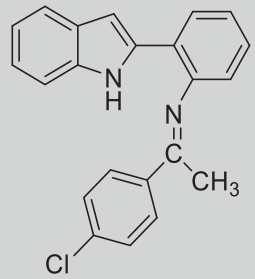

SMJ-2

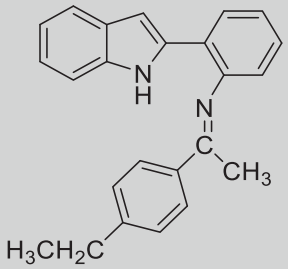

SMJ-4

Strain	SMJ-2 MIC (μg mL^{-1})	SMJ-4 MIC (μg mL^{-1})	Oxacillin MIC (μg mL^{-1})	Vancomycin MIC (μg mL^{-1})	Ciprofloxacin MIC (μg mL^{-1})	Erythromycin MIC (μg mL^{-1})
Staphylococcus aureus						
S. aureus SA-1199B	2	4	≤1	2	8	16
ATCC 29213 (MSSA)	2	4	0.25	1	0.5	0.25
ATCC 25923 (MSSA)	1	1	≤1	≤1	≤1	0.125
ATCC 43300 (MRSA)	2	4	64	1	≤1	0.25
ATCC 33591 (MRSA)	2	4	>128	1	0.5	>128
ATCC-BAA-1717 (MRSA)	2	4	128	1	≤1	>256
ATCC-BAA-39* (MRSA)	2	4	64	1	8	>256
GMCH 839 (MRSA)	2	16	2	1	8	>128
GMCH 4241 (MSSA)	1	4	≤1	≤1	16	>128
GMCH 6188* (MRSA)	1	2	>128	2	8	>500
GMCH 6187* (MRSA)	2	2	>128	≤1	16	64
GMCH 6152 (MRSA)	1	2	16	2	32	≤1
GMCH 3939* (MRSA)	2	16	4	1	>16	>128
GMCH 6022 (MRSA)	2	16	4	≤1	128	4
MRSA-1*	1	1	4	1	8	>500
MRSA-2*	1	16	4	1	8	>128
MRSA-3*	2	2	4	1	8	>500
MRSA-4*	1	16	4	1	32	>128
Enterococcus faecium						
ATCC 51559* (VRE)	2	2	>128	500	8	128
ATCC 19434*	2	4	8	≤1	32	128
Enterococcus faecalis						
ATCC 29212	2	2	8	2	≤1	32
ATCC 51299* (VRE)	0.25	0.25	32	128	≤1	≥128
Bacillus subtilis						
ATCC-6633	2	4	≤1	≤1	≤1	>128
MTCC-121	2	4	≤1	≤1	2	>128
Streptococcus mutans						
MTCC 497	2	4	≤1	2	≤1	>128
Escherichia coli						
ATCC 25922	≥64	≥64	64	128	≤1	>128
ATCC BAA 2774	≥64	≥64	>128	>128	>128	>128
Pseudomonas aeruginosa						
ATCC BAA 2795	≥32	≥32	>128	>128	>128	>128
Acinetobacter baumannii						
ATCC 19606	≥16	≥16	≥128	≥128	≤1	>128

(*) Indicates multidrug-resistant strain.
MSSA Methicillin-sensitive *Staphylococcus aureus*, *MRSA* Methicillin-resistant *Staphylococcus aureus*, *VRE* Vancomycin resistant *Enterococcus faecium*/Vancomycin resistant *Enterococcus faecalis*.

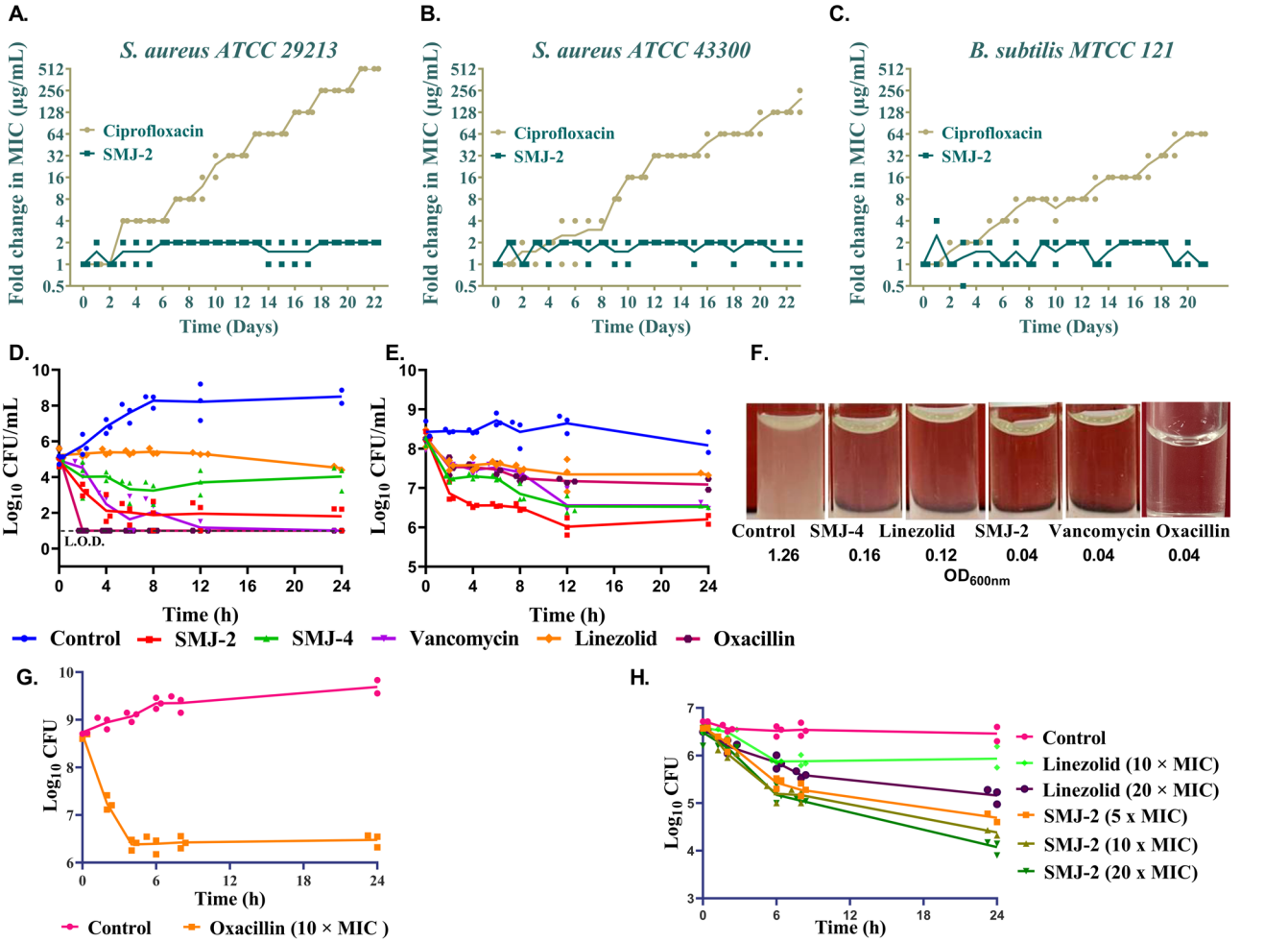

Fig. 1 | Time-dependent killing of pathogens by SMJ-2 and SMJ-4. A Evolution of resistant mutants of SMJ-2 (blue) and ciprofloxacin (brown) in cation-adjusted broth on *S. aureus* ATCC 29213, **B** *S. aureus* ATCC 43300, and (**C**) *B. subtilis* MTCC 121. Cells were passaged every 24 h. **D**, **E** Time-kill kinetic assay of SMJ-2 and SMJ-4 on *S. aureus* ATCC-MRSA-43300 in logarithmic and stationary phase respectively, the concentration of SMJ-2, SMJ-4, vancomycin, linezolid, and oxacillin at 10 × MIC. MIC of SMJ-2, SMJ-4, vancomycin, linezolid, and oxacillin were 2, 4, 1, 2, and 64 µg mL^{-1} respectively; (L.O.D. = Limit of Detection), **F** Photographic representation of SMJ-2, SMJ-4, vancomycin and linezolid treatment on *S. aureus* ATCC-MRSA-43300 in logarithmic phase, **G** Oxacillin treatment to *S. aureus* ATCC-29213 form persister cells, **H** Persister killing assay in the presence of SMJ-2 at 5 × MIC, 10 × MIC, and 20 × MIC and linezolid was used as positive control at 10 × MIC, and 20 × MIC. Experiments (**A**–**C**) represent two individual repeats ($n = 2$ biologically independent experiments), **D**, **E**, **G**, and **H** represent three individual repeats ($n = 3$ biologically independent samples), and the results correspond to average ± standard deviation.

SMJ-4 disturb which component of membrane potential, we used potentiometric fluorophore 3,3'-Dipropylthiadicarbocyanine Iodide [DiSC3(5)]. We used valinomycin and nigericin as positive controls to measure if the change in membrane potential is due to electrical potential ($\Delta\Psi$) or a change in pH (ΔpH). In response to the PMF's component ($\Delta\Psi$), DiSC3(5) builds up in the cytoplasmic membrane and self-quenches its fluorescence[12]. Valinomycin alters the electrical membrane potential and releases DiSC3(5) from the membrane, increasing fluorescence. Therefore, we exposed the bacterial cells to various concentrations of SMJ-2 in a dose-dependent manner, and we noticed a rapid drop in DiSC3(5) fluorescence, which suggested that SMJ-2 specifically destroyed the ΔpH component of the PMF similar to that of the positive control nigericin (Fig. 2A). We also conducted fluorescence measurements of the experiment without bacterial cells (using only buffer along with the dye and compounds) to preemptively eliminate any potential false positive results. Interestingly, we observed no alterations in fluorescence levels when utilizing compounds SMJ-2 and SMJ-4 in conjunction with DiSC3 dye. We also performed a membrane permeability assay and found that SMJ-2 does not permeabilize the bacterial membrane (Supplementary Fig. 9C).

Next, as PMF and ETC are interlinked, we looked into how the membrane potential dissipation caused by SMJ-2 and SMJ-4 affects respiratory adenosine triphosphate (ATP) synthesis. Dissipation of this electrochemical gradient should stop ATP production because the F_0F_1-ATPase uses the PMF to produce the energy. A bioluminescence assay determined ATP concentrations at the individual drugs' MIC values. In comparison to the control, intracellular ATP levels were significantly reduced at 5× and 10 × MIC with the addition of SMJ-2 and at 1×, 5×, and 10 × MIC of SMJ-4 (Fig. 2B).

Also, we wanted to check if SMJ-2 targets any cellular pathways in the bacteria because SMJ-2 has a low frequency of resistant mutant generation in vitro. Therefore, to elucidate if there is any cellular target, we used RNA sequencing to comprehend the physiology of *S. aureus* response to SMJ-2. Whole-transcriptome sequencing was carried out, and the hierarchical clustering of the data of all the samples was performed (Fig. 3A, B). The RNA sequencing data proves that SMJ-2 down-regulates genes involved in aminoacyl-tRNA biosynthesis (*ileS*, *gatB*), suggesting that SMJ-2 also inhibits bacterial growth at the translational level (Fig. 3C). We cross-validated the results, checked the mRNA expression of *ileS* and *gatB* genes, and found similar results, i.e., down-regulation of both genes was observed

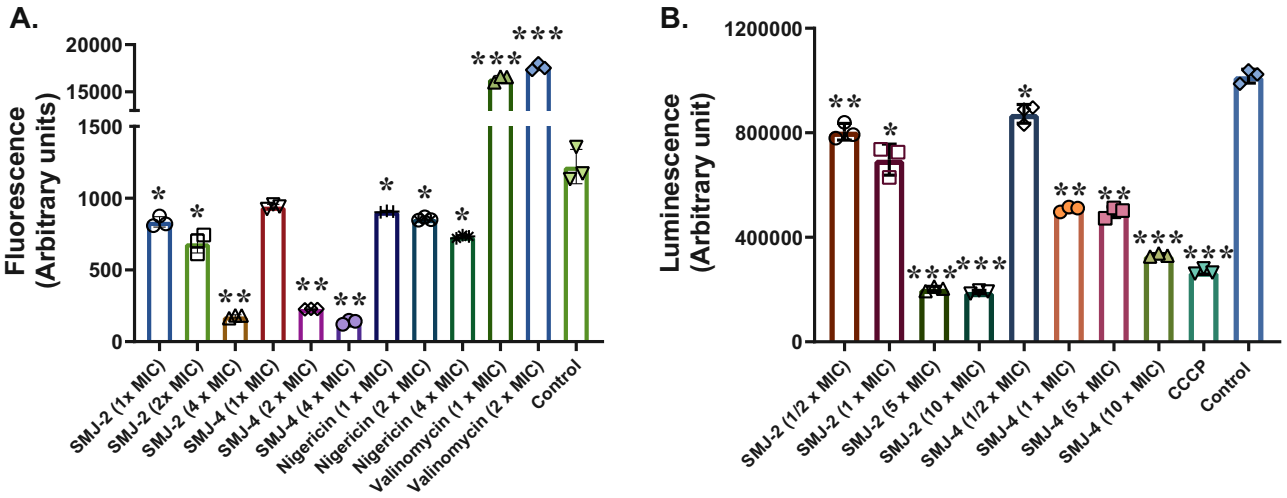

Fig. 2 | SMJ-2 and SMJ-4 disturb the membrane potential and adenosine triphosphate (ATP) pool. A SMJ-2 and SMJ-4 dissipate the ΔpH component of the proton motive force (PMF); 3,3'-Dipropylthiadicarbocyanine Iodide [DiSC3(5)] membrane depolarization assay, fluorescence in *S. aureus* ATCC 29213 upon exposure to SMJ-2, SMJ-4, and valinomycin and nigericin were used as positive controls that dissipate electric potential (ΔΨ) and pH (ΔpH) component of the PMF and dimethyl sulfoxide (DMSO) was used as negative control, MIC of nigericin is 0.0625 μg mL^{-1} and valinomycin is 64 μg mL^{-1}, **B** A bioluminescence test was used to determine the impact of SMJ-2 and SMJ-4 on intracellular ATP levels. The findings of each experiment are the average standard deviation of three individual repetitions ($n = 3$ biologically independent samples). Results were marked as significant (*) when $P < 0.05$ and highly significant (**) when $P < 0.01$, (***) when $P < 0.001$, and (****) when P value < 0.0001, and (ns) means non-significant. P value was calculated using a 95% class interval and paired t-test.

in SMJ-2 treated cells compared to untreated cells. These results indicate that SMJ-2 has multiple interlinked targets in bacteria, preventing the formation of resistant mutants in vitro.

We also noticed a down-regulation of the genes responsible for producing pantothenate (*panC, panB*) and Coenzyme A (CoA) (*CoaD*). Pantothenate is accountable for the synthesis of CoA[13,14]. Low CoA will lead to reduced acetyl-CoA formation (Supplementary Fig. 10). A decrease in acetyl-CoA generation would slow the tricarboxylic acid (TCA) cycle, which is essential for aerobic organisms' ability to produce energy and synthesize biosynthetic precursors[15].

We also observed increased NADH/H+ accumulation following treatment with SMJ-2 and SMJ-4. This accumulation is likely a result of NDH-2 inhibition, as NDH-2 typically converts NADH to NAD + . Consequently, when NDH-2 is inhibited, it fails to carry out this conversion, resulting in NADH buildup within the cell (Fig. 4A). NDH-2 is essential for bacteria's respiratory metabolism, and NDH-2 was also reported to contribute to biofilm formation and virulence[16,17]. As a result of the decrease in acetyl-CoA generation and NADH/H+ accumulation, the entire respiratory metabolism is hindered.

We, therefore, estimated cellular $NADH/H^+$ levels in the presence of SMJ-2 and SMJ-4 in the cellular bioenergetics state and observed that SMJ-2 and SMJ-4 showed an increase in accumulation of NADH/H+ levels with their increasing concentrations similar to the positive control polymyxin B[18,19] (Fig. 4A). In the respiratory system of numerous organisms, NDH-2 plays a crucial role; it maintains the balance of NAD^+ and NADH inside cells and acts as the entry site for electrons into the ETC to produce ATP[20]. NDH-2 assists in retaining the NADH/NAD^+ redox balance, catalyzes the transfer of electrons from NADH via flavin adenine dinucleotide (FAD) to membrane-bound quinone, and indirectly contributes to the production of PMF (Fig. 5). Now, we wanted to check if SMJ-2 is inhibiting the activity of NDH-2; therefore, we studied the expression of *ndh-2* in the presence of SMJ-2 treated and untreated *S. aureus* 29213, and we found down-regulation in mRNA expression of SMJ-2 treated sample (Fig. 4B).

We then evaluated the influence of our compounds SMJ-2 and SMJ-4 on the energetic state of *S. aureus* cells by assessing their impact on the reduction of iodonitrotetrazolium chloride (INT), an artificial electron acceptor. The electrons in the bacterial respiratory chain can convert the tetrazolium salt INT to a red insoluble formazan. Overall, SMJ-2 significantly reduced the reduction of INT to its formazan product by 98.73%, 54.63%, and 40.35%, and SMJ-4 reduced by 64.20%, 56.04%, and 56.38% when tested at 1×, 5×, and 10 × MICs compared to the untreated control, indicating that the cytoplasmic membrane's ability to transport electrons was compromised (Fig. 4C).

The RNA sequencing results also reveal the inhibition in alanine, aspartate, and glutamate metabolism (Fig. 3B), which is ultimately linked with Krebs cycle intermediates oxaloacetic acid and succinate[21]. Aspartate and glutamate are acidic amino acids, and their inhibition in the cytosol of bacteria increases the positive charge in the cytosol, ultimately disturbing the bacterial cell's membrane potential. We reasoned that, given the close relationship between PMF and the ETC, wherein the extrusion of protons by the ETC results in the generation of an electrochemical proton gradient, the dissipation of this gradient across the cytoplasmic membrane should eventually affect electron transport across the respiratory chain. The findings support the notion that focusing on bacterial PMF may be a clever way to combat the issue of rising antibiotic resistance.

The results demonstrate that SMJ-2 completely pounces the respiratory metabolism, which results in cell death, and all the results are efficiently interlinked.

SMJ-2 does not inhibit the cell division activity of bacteria

In literature, indole-based compounds have been reported to inhibit bacterial growth by targeting cell division and FtsZ[22]. Therefore, we treated *B. subtilis MTCC* 121 with 0.5 × MIC of SMJ-2. If FtsZ had been the target of SMJ-2, then an elongation of *B. subtilis* would have occurred, but no such results were observed that indicate SMJ-2 does not inhibit cell division or FtsZ (Supplementary Fig. 11).

SMJ-2 treatment inhibits staphyloxanthin synthesis and increases the production of ROS, sensitizing the bacteria against hydrogen peroxide (H_2O_2)

Staphyloxanthin and its metabolic intermediates were quantified in the presence and absence of SMJ-2 and SMJ-4. All intermediaries evaluated, including 4, 4-diapophytoene, 4, 4-diaponeurosporene, 4, 4-diaponeurosporenic acid, and staphyloxanthin, showed a significant reduction in spectrometric measurements of staphyloxanthin biosynthesis pathway

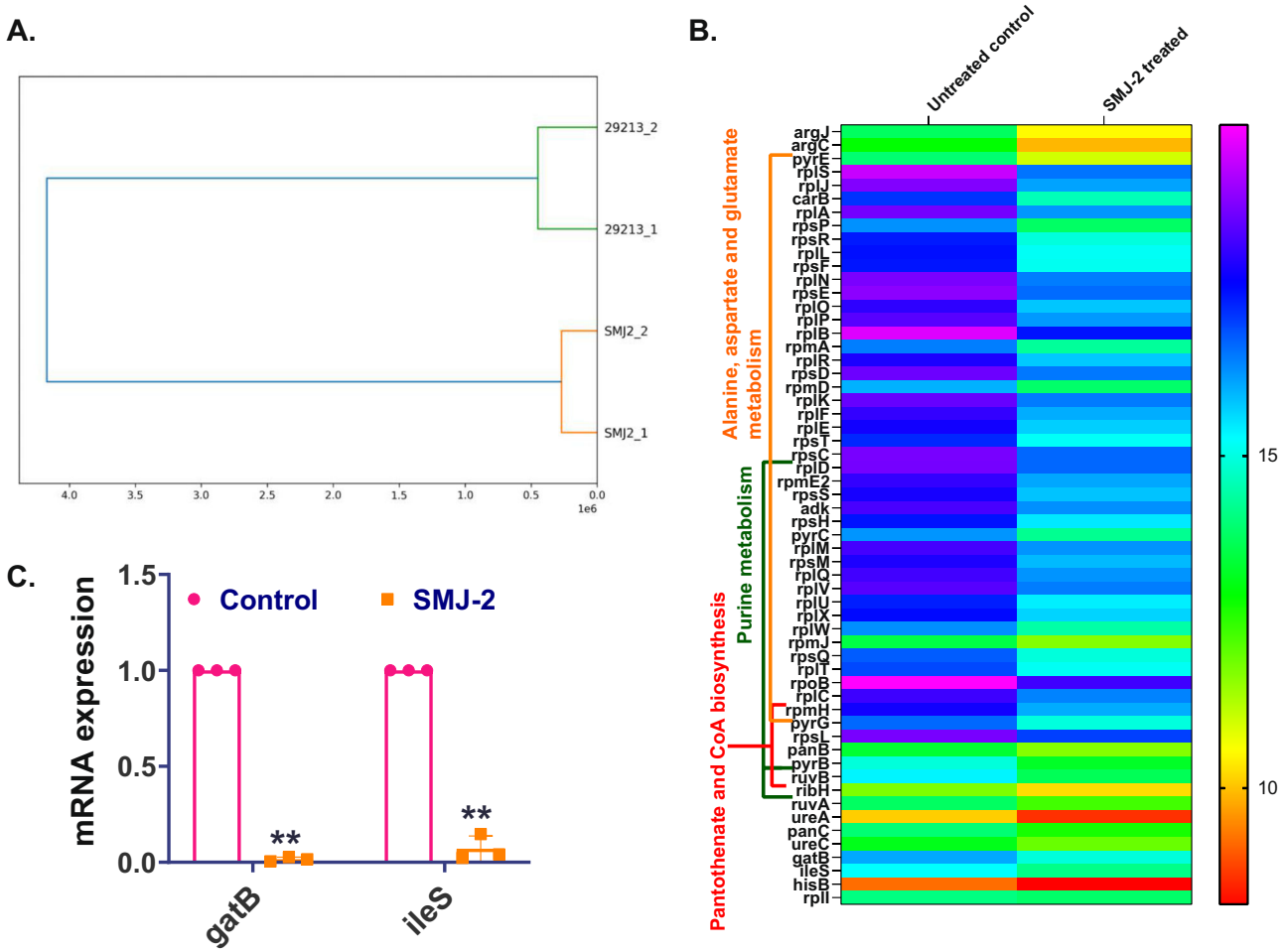

Fig. 3 | Transcriptomic study of SMJ-2 treated and untreated bacterial cells. **A** The hierarchical clustering of the data for *S. aureus* ATCC 29213 untreated and SMJ-2 treated samples, **B** Heat Map of relative gene expression of *S. aureus* ATCC 29213 treated with SMJ-2 obtained from RNA sequencing. Given are the two biological replicates of SMJ-2 treated cells relative to untreated control on a $\log_2$-fold scale, **C** *mRNA* expression of *gatB* and *ileS* gene of SMJ-2 treated and untreated control set. Experiments (**A**), (**B**), and (**C**) represent two individual repeats ($n = 2$ biologically independent samples).

metabolic intermediates (Fig. 6A–D). Production of ROS is substantially enhanced by a drop in [NAD^+] and an increase in the NADH/NAD^+ ratio[23]. ROS formation depends on nucleotide concentrations and the NADH/NAD^+ ratio because only the reduced flavin's nucleotide-free binding site can react with oxygen[23]. It's been established that cellular respiration is necessary for staphyloxanthin synthesis[24]. A drop in staphyloxanthin after exposure to SMJ-2 and SMJ-4 will demonstrate how it affects the staphyloxanthin-producing bacteria's ability to withstand ROS. According to the ROS quantification assay results, treated samples had fluorescence intensities nearly 2.5 times higher than controls at 1 h after treatment with the DCFH2-DA dye, indicating that more ROS had been generated than in untreated bacterial samples. The SMJ-2 and SMJ-4 treatments reduced staphyloxanthin resistance and caused an increase in the quantity of ROS produced in the singlet oxygen assay (Fig. 6E).

H_2O_2 treatment on untreated control cells and SMJ-2 and SMJ-4 were used to test this theory. Photos of H_2O_2 diffusion assay plates demonstrated how the clearance zone gradually increased when SMJ-2 and SMJ-4 concentrations increased in TSA plates compared to the control plate. At 0.75 × MIC and 0.5 × MIC, respectively, SMJ-2 showed a zone of 25 mm and 24 mm, while SMJ-4 showed a 23 mm and 22 mm zone. A 21 mm zone was visible in the untreated control. The positive control miconazole showed zones of 23 mm and 22 mm (Fig. 6F). Since miconazole suppresses the formation of biofilms, staphyloxanthin synthesis, and other virulence factors, we have utilized it as the positive control[25].

SMJ-2-treated bacteria are susceptible to oxidative stress and sensitive to the host immune system

Our in vitro findings show that the staphyloxanthin produced by *S. aureus* is essential and sufficient to foster oxidative resistance. We employed a mouse subcutaneous paradigm model to determine the importance of these observations on disease development. Individual animals were infected with the untreated and SMJ-2 pre-treated bacterial suspensions. Bacterial suspension that had been pre-treated with miconazole[26] served as the positive control. We took two untreated groups; one was sacrificed at the end of 24 h (to check the maximum bacterial load) and the other at the end of 96 h with different treatment groups (for comparison). At the end of 24 h, the untreated control group's bacterial burden had reached approximately 8.98 $\log_{10}$ CFU/gm skin.

In contrast, at the end of 96 h, the untreated control group had self-recovered by 1.05 $\log_{10}$, leaving 7.93 $\log_{10}$ CFU/gm skin. However, SMJ-2 demonstrated a self-recovery by 2.07 $\log_{10}$ that produced 6.91 $\log_{10}$ CFU/gm skin, even better than the positive control miconazole that showed a self-recovery by 1.8 $\log_{10}$ that produced 7.18 $\log_{10}$ CFU/gm skin (Fig. 6G). Qualitative analysis of skin lesions consistently showed better recovery in the treated group than in the untreated mice group (Fig. 6H).

SMJ-2 inhibits biofilm formation and actively eradicates the pre-formed biofilm

In hospitals, patients are vulnerable to pathogens that develop biofilms, and *S. aureus* is one of the most common pathogens to cause infections related to

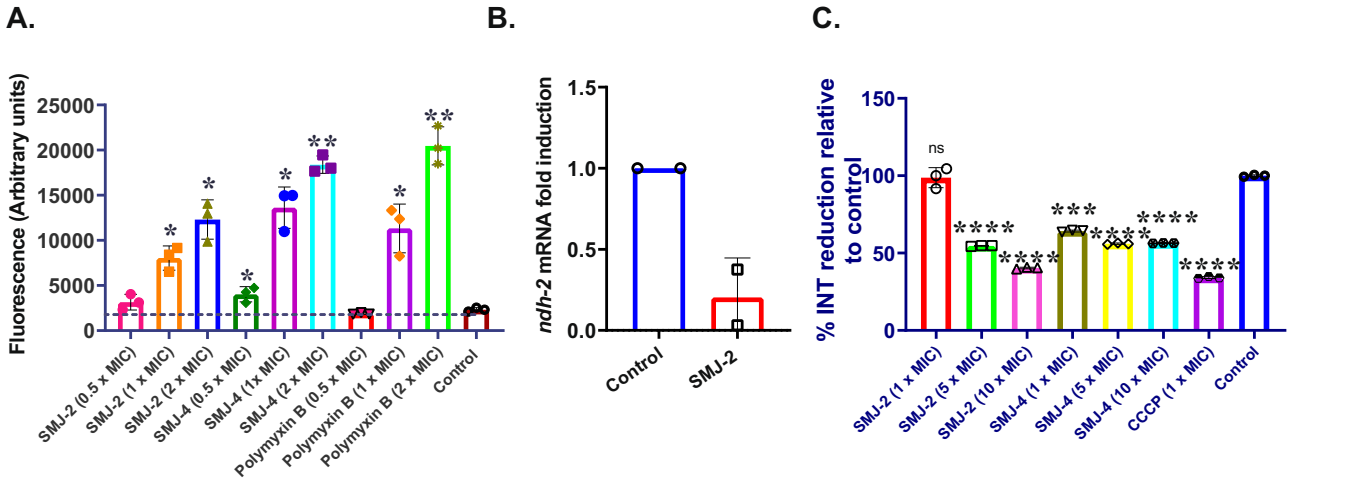

Fig. 4 | Effect of SMJ-2 on respiratory metabolism. A Increased resorufin fluorescence following treatment shows the accumulation of NADH/H+ in *S. aureus* ATCC 29213; values are in relation to the control, polymyxin B was used as positive control, and its MIC is 32 μg mL^{-1}. **B** *mRNA* expression of *ndh-2* gene in SMJ-2 treated and untreated sample of *S. aureus* 29213 strain, **C** Effects of SMJ-2, SMJ-4, and carbonyl cyanide m-chlorophenylhydrazine (CCCP) on the breakdown of iodonitrotetrazolium chloride (INT) into its detectable formazan product with a 490 nm absorbance. CCCP, a known electron uncoupler, was used as a positive control; the MIC of CCCP is 0.5 μg mL^{-1}. The findings of each experiment are the average standard deviation of three individual repetitions ($n = 3$ biologically independent samples). Results were marked as significant (*) when $P < 0.05$ and highly significant (**) when $P < 0.01$, (***) when $P < 0.001$, and (****) when P value < 0.0001, and (ns) means non-significant. P value was calculated using a 95% class interval and paired t-test.

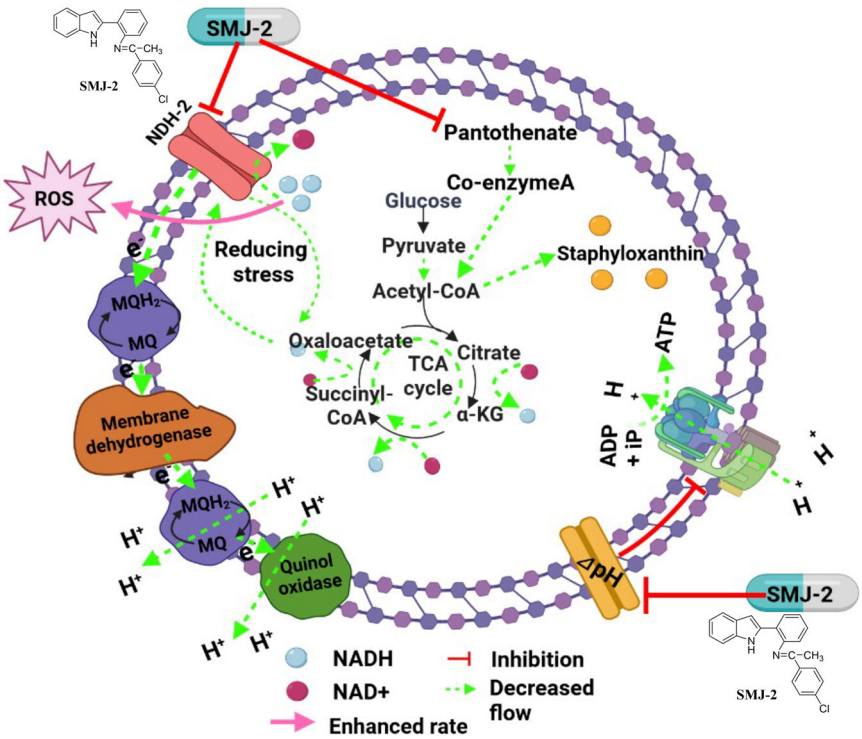

Fig. 5 | Schematic diagram of the mechanism of action of SMJ-2. Created in BioRender. Tambat, R. (2024) BioRender.com/g55n399.

medical care[27]. We evaluated SMJ-2 and SMJ-4's anti-biofilm activity against the *S. aureus* ATCC 29213 and *S. aureus* GMCH 839 strain. SMJ-2 inhibited 8.86%, 39.69%, and 36.76% of the biofilm formation in the crystal violet assay, whereas SMJ-4 inhibited 12.23%, 19.77%, and 82.97% of the biofilm and ciprofloxacin 10.89%, 68.54%, and 92.80% at 1/8×, 1/4×, and 1/2× MIC, respectively on *S. aureus* ATCC 29213 (Fig. 7A). SMJ-2 inhibited 3.72%, 32.04%, and 38.69% of the biofilm formation in the crystal violet assay, whereas SMJ-4 inhibited 15.4%, 22.36%, and 46.14% of the biofilm at 1/8×, 1/4×, and 1/2 × MIC and ciprofloxacin inhibited 14.49%, and 13.23% at 1/4×, and 1/2 × MIC, respectively on *S. aureus* GMCH 839 (Fig. 7D). SMJ-2 eradicated 47.3%, 49.5%, and 60.27% of the pre-formed biofilm in the crystal violet assay, whereas SMJ-4 eradicated 11.22%, 35.72%, and 46.9% of the biofilm at 4×, 8×, and 16 × MIC and ciprofloxacin eradicated 20.05%, 20.65%, and 36.42% at 4×, 8×, and 16 × MIC, respectively on *S. aureus* ATCC 29213 (Fig. 7B). It's noteworthy that when we checked the biofilm eradication on pre-formed biofilms, we found that SMJ-2 eliminated 79.06%, 77.04%, and 80.61% of the biofilms. In comparison, SMJ-4 eliminated 36.48%, 73.7%, and 79.45%, and ciprofloxacin inhibited 31.36%,

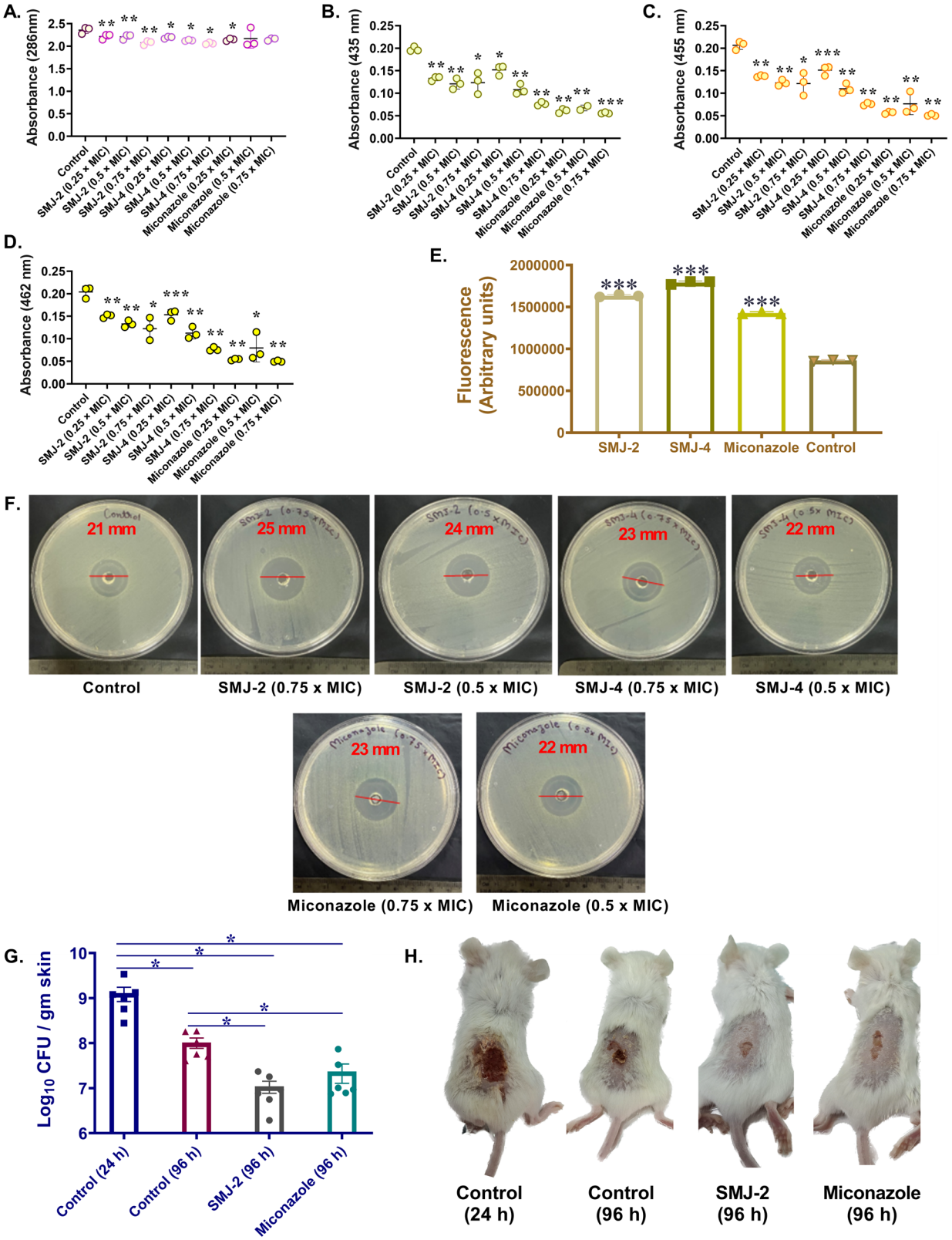

45.98, and 44.24% of the biofilms at 4×, 8×, and 16 × MIC, respectively on *S. aureus* GMCH 839 (Fig. 7E). To further examine the viability of surviving biofilm-forming bacteria following biofilm eradication by SMJ-2, SMJ-4, and 3-(4, 5-dimethylthiazol-2-yl)-2, 5-diphenyl tetrazolium bromide (MTT) was used. At 4×, 8×, and 16 × MIC, respectively, we discovered 79.96%, 83.64%, and 88.62% viable biofilm eradication by SMJ-2 and 53.97%, 75.11%, and 81.84% viable biofilm eradication by SMJ-4 and 61.15%, 70.5%, and 69.01% viable biofilm eradication by ciprofloxacin on *S. aureus* ATCC 29213 (Fig. 7C). At 4×, 8×, and 16 × MIC, respectively, we discovered 70.03%, 71.62%, and 81.46% viable biofilm eradication by SMJ-2 and 53.73%, 72.58%, and 65.71% viable biofilm eradication by SMJ-4 on *S. aureus* GMCH 839 (Fig. 7F). We confirmed the biofilm eradication ability

Fig. 6 | Staphyloxanthin inhibition causes oxidative stress on bacteria. **A** Spectrometric quantification of staphyloxanthin intermediates, namely 4,4-diapophytoene (286 nm), **B** 4,4-diaponeurosporene (435 nm), **C** 4,4-diaponeurosporenic acid (455 nm) and (**D**) staphyloxanthin (462 nm) extracted from control and SMJ-2, SMJ-4, and miconazole treated (0.75 × MIC, 0.5 × MIC) treated *S. aureus* ATCC 29213 cells, **E** measurement of the fluorescence intensity to quantify the amount of reactive oxygen species (ROS) produced in the singlet oxygen test in the presence and absence of SMJ-2, SMJ-4, and miconazole (0.5 × MIC), **F** *S. aureus* is exposed to SMJ-2 and SMJ-4 (0.75 × MIC and 0.5 × MIC, respectively), is more susceptible to H_2O_2 than the untreated control, according to a well-diffusion experiment, **G** Staphyloxanthin contributes to subcutaneous abscesses infection in mice. Mice were infected with SMJ-2 and miconazole-treated and untreated *S. aureus* ATCC 29213 strain on the skin lesions. The graph represents the CFU of SMJ-2 and miconazole treated and untreated *S. aureus* ATCC 29213 bacterial strain recovered from the skin lesion of each mouse in the groups ($n = 6$ biologically independent animals). **H** Photographic image represents mice from each group, control (24 h), control (96 h), SMJ-2 (96 h), and miconazole (96 h). Results were marked as significant (*) when $P < 0.05$ and highly significant (**) when $P < 0.01$, and (***) when $P < 0.001$. *P* value was calculated using a 95% class interval and paired *t*-test.

of SMJ-2 at 4× and 8× MIC by confocal microscopy on *S. aureus* GMCH 839 (Fig. 7G).

SMJ-2 shows a longer post-antibiotic effect (PAE) than other known antibiotics

The PAE of SMJ-2 and SMJ-4 were evaluated by subjecting an exponential-phase culture of *S. aureus* ATCC 29213 to 2 × MICs of SMJ-2, SMJ-4, ciprofloxacin, and vancomycin, which resulted in PAE values of 2, 1, 1.5, and 0.5 h. Compared to ciprofloxacin and vancomycin, SMJ-2 showed an increase in 0.5 and 1.5 h, whereas SMJ-4 showed an increase of 0.5 h more than vancomycin. The PAE results show that SMJ-2 has a longer post-antibiotic life than SMJ-4, ciprofloxacin, or vancomycin (Supplementary Fig. 13). When creating antibiotic dose regimens, PAE may be a crucial factor. Antibacterials with minimum or lower PAEs may require serum concentrations above MICs during treatment interval[28].

SMJ-2 and SMJ-4 show favorable in silico and in vitro physicochemical and absorption, distribution, metabolism, excretion, and toxicity (ADMET) properties

The drug-likeness of both compounds is found as per the Lipinski Rule of Five. The values of these physicochemical parameters, such as molecular weight, number of hydrogen bond donors, number of hydrogen bond acceptors, and number of rotatable bond values, were observed to be within the acceptable range according to Lipinski's rule. Lipinski's Rule of Five states that SMJ-2 and SMJ-4 have drug-likeness properties because these compounds violate only one parameter, i.e., log $P > 5$ (Supplementary Table 8).

According to the software, the Caco-2 permeability score should be > −5.15 log unit for the compound to be active, and SMJ-2 and SMJ-4 generated a score of −4.857 log unit and −4.882 log unit; this indicates the compounds show Caco-2 permeability. MDCK permeability is 8×10^{-6} and 9×10^{-6} for SMJ-2 and SMJ-4, respectively, that falls under the range of medium permeability, i.e., $2–20 \times 10^{-6}$ cm/s. SMJ-2 is neither a substrate nor an inhibitor of Pgp, while SMJ-4 is not a substrate but an inhibitor of Pgp.

Both compounds' F30% (bioavailability) is ≥30%, indicating their therapeutic activity. F30% signifies 30% oral bioavailability in humans, a crucial pharmacokinetic factor for orally administered drugs, as it measures drug delivery efficiency to the systemic circulation. The results can be interpreted as follows: F30%− (Category 0) compounds have a bioavailability of at least 30%, while F30%+ (Category 1) compounds have less than 30% bioavailability. The likelihood of a compound being F30%+ is expressed as a value between 0 and 1. According to the ADMET lab 2.0 prediction tool, values between 0-0.3 indicate excellent bioavailability, 0.3–0.7 indicate medium bioavailability, and 0.7–1 indicate poor bioavailability. Based on the structural moieties of the compounds, the ADMET lab 2.0 software has empirically determined that SMJ-2 and SMJ-4 fall into the excellent bioavailability category. Therefore, these compounds are likely to be therapeutically active.

Both compounds are unable to penetrate the blood-brain barrier. The human hepatotoxicity scores of SMJ-2 and SMJ-4 are 0.09 and 0.104; that means compounds are safe on hepatic cells according to the software analysis, and the clearance of both compounds from the system is 2.85 and 3.375 and clearance value < 5 mL min^{-1} kg^{-1} which is considered to be low.

The log *P* values obtained for SMJ-2 and SMJ-4 in the in silico ADMET analysis in ADMET lab 2.0 were within the range of 5–6. When performing the log P study during 24 h experiment, the compounds SMJ-2 and SMJ-4 were not detected in the aqueous phase, i.e., the compounds are moving into the organic phase, viz., *n*-octanol phase. Log P obtained during the 24 h experiment was within the range of 5–6, which is the same as in the in silico analysis.

The short half-life is a predictive statement obtained through the online free software, i.e., ADMET lab 2.0. It may or may not happen. The in vitro pKa of SMJ-2 and SMJ-4 was obtained at 5.16, which is quite possible as it is in the range of log *P* values.

The numbers in Supplementary Table 8 are the values predicted by the software for different physicochemical and ADMET parameters for SMJ-2 and SMJ-4. According to Lipinski's rule of five, the software provides a particular range of various physicochemical parameters for these two compounds to be called "drug-like candidates." If the values for the compounds fall within the range predicted for each parameter, then these can be considered a "drug-like candidate."

Solubility is a vital pre-formulation parameter contributing to the compound's absorption through biological membranes. The compound will be easily absorbed if it is in the solution form. The solubility data in Supplementary Table 9 shows that both SMJ-2 and SMJ-4 are majorly soluble in organic solvents. These compounds are very slightly soluble in water. For further drug development, various techniques can be implemented to improve the aqueous solubility of these two compounds, i.e., particle size reduction, pH adjustment, salt formation, etc. The oral and intestinal absorption of both SMJ-2 and SMJ-4 was good. SMJ-2 and SMJ-4 were soluble in ethyl acetate, chloroform, methanol, dimethyl sulfoxide, and diethyl ether (Supplementary Table 9).

The safety profile of SMJ-2 ex vivo and in vivo

Hemolytic activity was evaluated by measuring the release of hemoglobin from rabbit erythrocytes as a function of concentration. SMJ-2 and SMJ-4 demonstrated low hemolytic activity. SMJ-2 exhibited 23.64 ± 1.44% hemolysis up to 100 μg mL^{-1} concentration, that is, relatively high compared to the working concentration (Supplementary Fig. 14A). At the same time, SMJ-4 displayed a maximum of 5.93 ± 5.7% hemolysis at 100 μg mL^{-1} concentration. Mammalian cell viability assays were conducted on Human Embryonic Kidney Cells (HEK) and hepatoblastoma cell line (HepG2) using MTT assay at 2 to 100 μg mL^{-1} concentrations. In HEK, cell viability of 95.25 ± 0.36%, 96.46 ± 5%, and 93.16 ± 3.92% were observed at 100 μg mL^{-1} for SMJ-2, SMJ-4, and linezolid respectively (Supplementary Fig. 14B). In HepG2, cell viability of 74.56 ± 8.5%, 74.63 ± 5.14%, and 64.31 ± 7.44% were observed at 100 μg mL^{-1} for SMJ-2, SMJ-4, and linezolid respectively (Supplementary Fig. 14C). In THP-1, cell viability of 59.78 ± 5.54%, 62.82 ± 0.12%, and 73.88 ± 4.45% were observed at 100 μg mL^{-1} for SMJ-2, SMJ-4, and linezolid respectively (Supplementary Fig. 14D).

An adverse effect known as acute toxicity occurs within 7 days after a person takes a single or repeated dose of a medicine. Unwanted consequences might alter a person's general functioning or the functionality of particular organs by causing biochemical lesions and functional impairments in organs[29,30]. We looked into SMJ-2's in vivo acute toxicity to learn more about the compound's medicinal potential after seeing promising

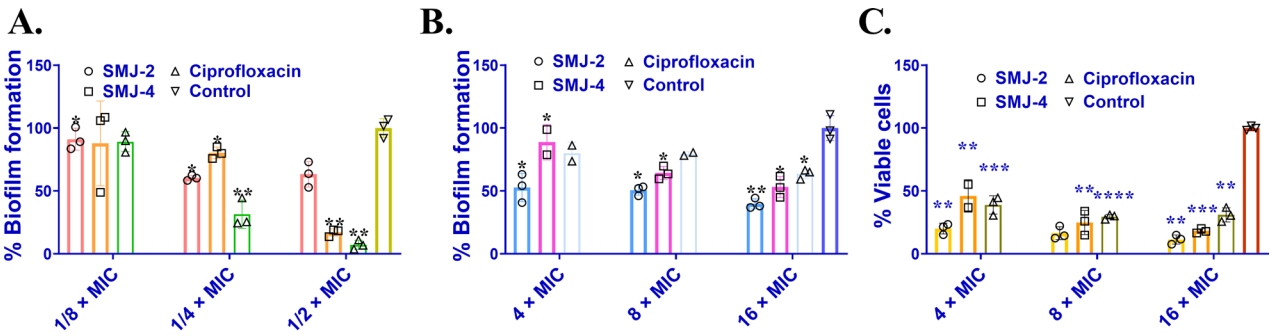

Bacterial strain used: *S. aureus* ATCC 29213

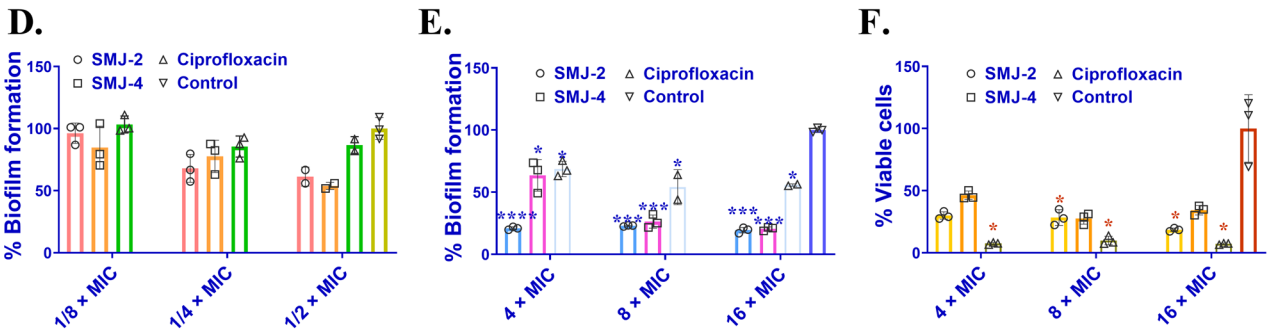

Bacterial strain used: *S. aureus* 839

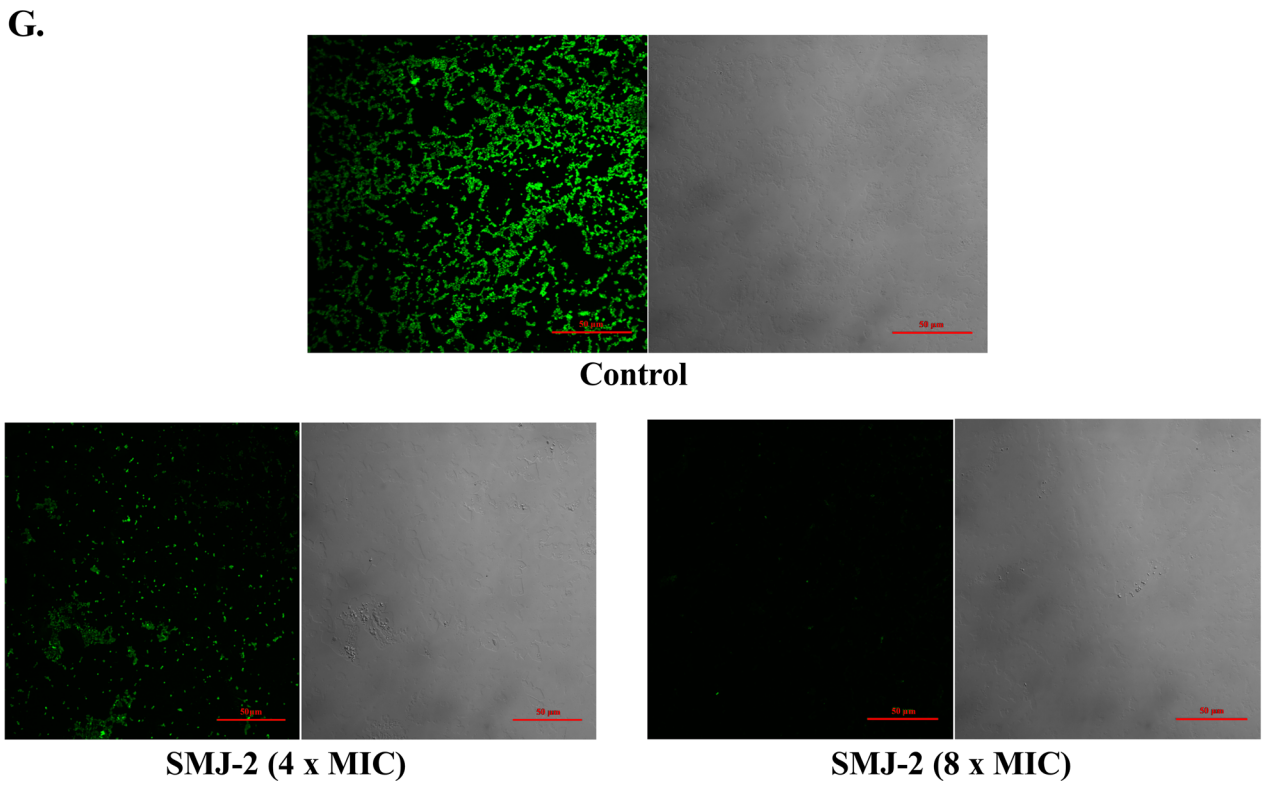

in vitro toxicity results on mammalian cell lines. Each mouse received oral administration of SMJ-2 at progressively higher dosages ranging from 20 to 500 mg kg^{-1} at each stage. No animal died while receiving SMJ-2, and 7 days later, neither body weight nor blood glucose levels had changed. With an LD_{50} of >500 mg kg^{-1}, SMJ-2 exhibits a high safety index. The treated mice displayed the same behavioral pattern as the control group. The mice were sacrificed for histological analysis (Fig. 8A), and blood was drawn for biochemical assays via the retro-orbital method. Similar outcomes to those of the control group were seen in histopathological examinations. When treated mice were tested for renal function, their blood urea and serum creatinine levels were normal, matching those of the control group. Bilirubin (total), bilirubin direct (conjugated), bilirubin indirect (unconjugated),

Fig. 7 | SMJ-2 effectively eradicates pre-formed biofilms. A Crystal violet % Biofilm inhibition of SMJ-2, SMJ-4, and ciprofloxacin at 1/8 × MIC, 1/4 × MIC, and 1/2 × MIC compared to untreated control on *S. aureus* ATCC 29213, **B** Crystal violet Biofilm eradication of SMJ-2, SMJ-4, and ciprofloxacin at 4 × MIC, 8 × MIC, and 16 × MIC compared to untreated control on *S. aureus* ATCC 29213, **C** Viable Biofilm cells of SMJ-2, SMJ-4, and ciprofloxacin at 4 × MIC, 8 × MIC, and 16 × MIC compared to untreated control on *S. aureus* ATCC 29213, **D** Crystal violet Biofilm inhibition of SMJ-2, SMJ-4, and ciprofloxacin at 1/8 × MIC, 1/4 × MIC, and 1/2 × MIC compared to untreated control on *S. aureus* 839, **E** Crystal violet Biofilm eradication of SMJ-2, SMJ-4 and ciprofloxacin compared to untreated control on *S. aureus* 839, **F** Viable Biofilm cells of SMJ-2, SMJ-4, and ciprofloxacin at 4 × MIC, 8 × MIC, and 16 × MIC compared to untreated control on *S. aureus* 839, **G** Confocal microscopy of biofilm eradication by SMJ-2 at 4 × MIC, and 8 × MIC on *S. aureus* 839, scale bar 50 µm. The findings of each experiment are the average standard deviation of three individual repetitions ($n = 3$ biologically independent samples). Results were marked as significant (*) when $P < 0.05$ and highly significant (**) when $P < 0.01$, and (***) when $P < 0.001$. P value was calculated using a 95% class interval and paired t-test.

serum glutamic oxaloacetic transaminase (SGOT)/aspartate aminotransferase (AST), and serum glutamic pyruvic transaminase (SGPT)/alanine aminotransferase (ALT) levels in the treated animals were all within normal ranges, according to the results of the liver function test (LFT) (Table 2).

SMJ-2 shows high efficacy in murine thigh infection

The in vitro drug efficacy inspired our evaluation of SMJ-2 in vivo. Mice were given 2.5×10^7 CFU of *S. aureus* ATCC-43300 infection intramuscularly. After 4 h, the first control group was sacrificed to see if the infection had been effectively established. The mice's right thighs were then homogenized and plated. Approximately 1.56×10^6 CFUs were discovered in the control group's sacrificed tissue at 4 h. SMJ-2 treatment 4 h after infection was highly effective, with 1.005 $\log_{10}$ and 3.874 $\log_{10}$ reductions compared to untreated control groups after 4 and 24 h, respectively. Compared to 4 and 24 h of untreated control, linezolid given as positive control showed a reduction of 0.978 $\log_{10}$ and 3.847 $\log_{10}$ (Fig. 8B).

SMJ-2 shows a high survival rate in the murine peritonitis model

A compelling investigation was conducted using a mouse peritonitis model. Mice were intraperitoneally injected with 500 µL of 2×10^7 CFU mL^{-1} of *S. aureus* ATCC-43300, a dosage that results in 90% mortality, to cause septicemia. At 1, 3, and 5 h after infection, 200 µL of SMJ-2 (20 mg kg^{-1}) prepared in sunflower oil was given orally thrice daily. Mice treated with SMJ-2 showed a 90% survival rate, while the mice group treated with linezolid had a 100% survival rate (Fig. 8C).

Discussion

Antibiotic resistance is a growing concern in modern medicine, as the overuse and misuse of antibiotics have led to resistance in bacteria[31]. Gram-positive bacteria, such as MRSA and VRE, are major causes of human bacterial infections[31]. Teixobactin, a new antibiotic reported in 2015, was very effective against gram-positive bacteria, which contained an unusual depsipeptide containing enduracididine, methyl phenylalanine, and four D-amino acids. The drawback of this natural antibiotic was its difficulty in synthesis because of the unusual depsipeptide. A phase II trial for the synthetic FabI inhibitor afabicin, which targets gram-positive *S. aureus*, is underway. FabI is a crucial enzyme in the fatty acid production pathway[32]. But there may be a problem with this single-target antibiotic developing resistance[1]. The development of daptomycin was initially halted due to myopathy concerns, but it resumed in 1997 when Cubist Pharmaceuticals Inc. licensed it. A once-daily dosing regimen was later found to mitigate side effects without compromising efficacy[33].

In this study, we used a combination of chemical synthesis and screening assays to discover a new antibacterial moiety, SMJ-2, with potent activity against gram-positive bacteria. The discovery of new chemically synthesized antibacterial compounds targeting gram-positive bacteria significantly contributes to the antibiotic discovery field. Chemical synthesis allows researchers to design and optimize compounds for potency and selectivity, leading to the discovery of a lead compound with potent activity against a broad range of gram-positive bacteria. We also discuss the wide range of activity against gram-positive bacteria, including action against MRSA, VRE, and many clinical isolates, all of which are high-priority pathogens according to the WHO. Unlike ciprofloxacin, we also show that repeated exposure of SMJ-2 to bacteria at concentrations below the inhibitory threshold does not confer resistance. This confluence of characteristics makes conducting more research on these understudied compounds compelling.

SMJ-2 was surprisingly found to be equally active on logarithmic phase cells, stationary phase cells, and persister cells of *S. aureus*. Since bacterial cells need a constant electrochemical transmembrane gradient to thrive and the disturbance in the PMF would result in the death of persister cells, indicates SMJ-2 may target the PMF[11]. SMJ-2 was found to disturb the membrane potential, disrupting the ETC pool and depletion of intracellular ATP. We also performed RNA sequencing to get an insight into the deep mechanism of action of the antibacterial compound SMJ-2.

We found that genes involved in pantothenate (*panC, panB*) and CoA (*CoaD*) synthesis were down-regulated upon exposure to SMJ-2 at sub-inhibitory concentration. The primary precursor for the production of CoA is pantothenate. A reduced rate of CoA synthesis results in decreased acetyl-CoA production slows the TCA cycle, and impairs respiratory metabolism. Furthermore, SMJ-2 was found to suppress the expression of the *ndh-2* gene, thereby inhibiting the activity of NDH-2, a key enzyme in respiratory metabolism that contributes indirectly to PMF generation. NDH-2s are an appealing pharmacological target since they are only found in bacteria, fungi, protozoan mitochondria, and some plants, but not in mammals[9]. The inhibition of TCA and NDH-2 by SMJ-2 leads to an accumulation of NADH and a reduction in NAD+. The decreased NAD+ levels result in increased ROS production[23]. Consequently, SMJ-2 effectively halts respiratory metabolism, causing cell death. This interconnection of targets demonstrates that inhibiting one component can lead to the collapse of the entire metabolic machinery.

The other aspect of inhibition of the TCA cycle and CoA leads to the inhibition of staphyloxanthin pigment. As CoA biosynthesis declines, less acetyl-CoA is produced, inhibiting the mevalonate pathway and lowering farnesyl diphosphate production[34, 35]. It is known that the generation of staphyloxanthin depends on farnesyl diphosphate[35]. Staphyloxanthin, a known virulence factor in *S. aureus*, promotes resistance to ROS and the host immune system. Reduction in staphyloxanthin and production of ROS makes the bacteria susceptible to the singlet oxygen produced by H_2O_2. By causing oxidative damage to bio-compounds, ROS can kill pathogens directly, or they can kill them indirectly by promoting pathogen eradication through a variety of non-oxidative mechanisms, including pattern recognition receptor signaling, autophagy, by forming neutrophil extracellular traps, and T-lymphocyte responses. Hence, the suppression of ROS generation should be expected to increase infection[8].

In silico and in vitro physicochemical properties revealed that SMJ-2 and SMJ-4 follow the Lipinski rule. One exciting observation was that in the in silico study, the log P value was high, indicating the compounds' lipophilic character of the compounds, while the in vitro study revealed that at the end of 48 h, log P value decreased, which means the compounds shifted towards the hydrophilic side. The in silico Caco-2 permeability and human intestinal absorption were favorable; compounds did not cross the blood-brain barrier, indicating favorable absorption and distribution of SMJ-2. SMJ-2 inhibited pre-formed biofilm and was proven safe in hemolysis and in vitro cytotoxicity studies on HEK, HepG2, and THP-1 cells. SMJ-2 was efficacious in the in vivo mouse thigh infection model and showed 90% survival in the mouse peritonitis model. It was found to be safe at 500 mg kg^{-1} in acute toxicity studies.

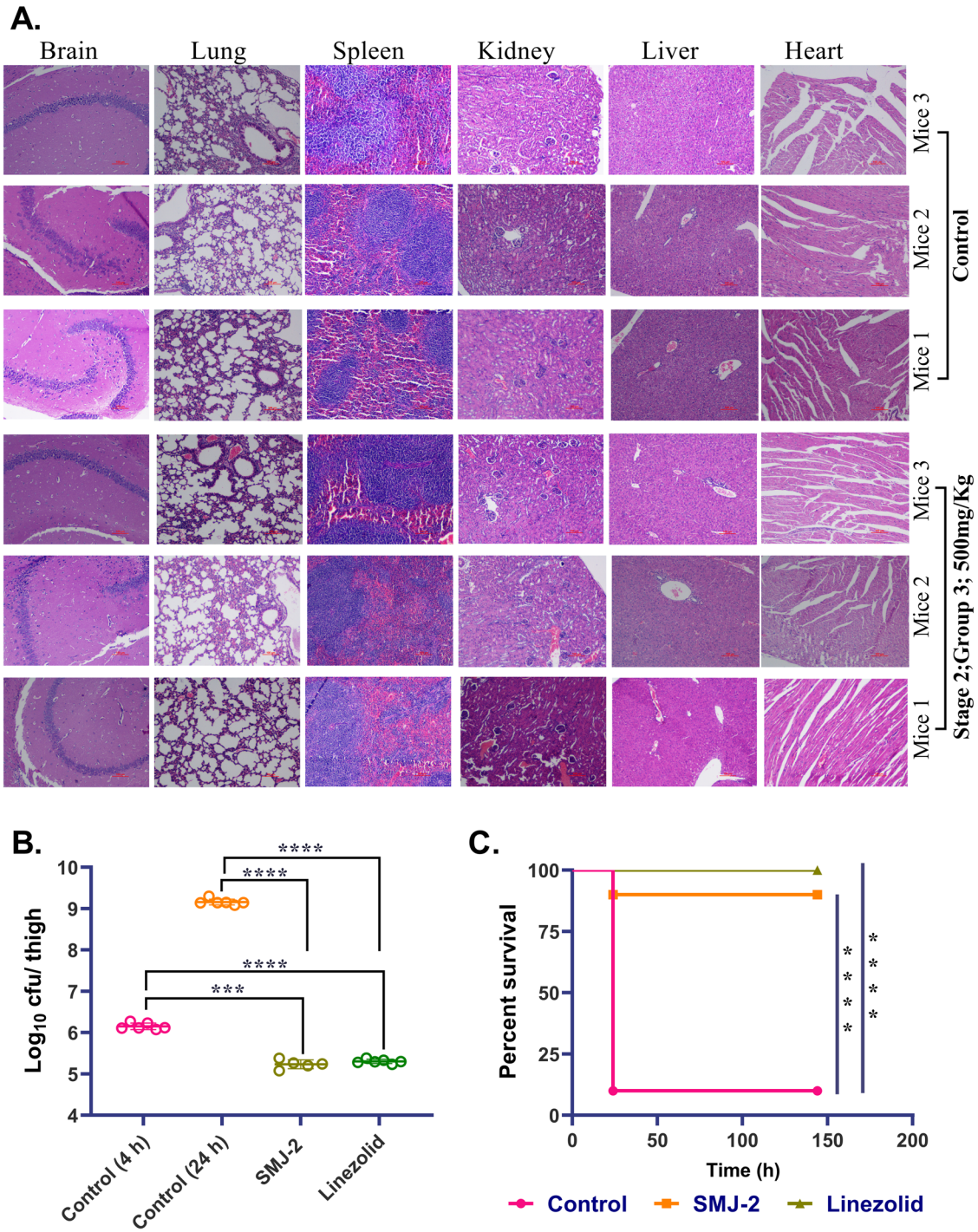

Fig. 8 | SMJ-2 is safe and efficacious in mice models. A Histopathological analysis of 6 major organs of BALB/c mice after subcutaneous administration of SMJ-2 at 500 mg kg^{-1} and control after 7 days of administration, scale bar 100 µm, **B** Neutropenic mouse thigh infection model: Single oral dose treatment (20 mg kg^{-1} SMJ-2; 6 mice per group ($n = 6$); 4 h after infection). CFU was determined 24 h post-infection for SMJ-2 and linezolid-treated mice and untreated controls; CFU was calculated 4 and 24 h post-infection, and significance was calculated by comparing to 24 h control. **C** Mouse peritonitis survival model: Three oral dose treatments (40 mg kg^{-1} SMJ-2 and positive control linezolid 40 mg kg^{-1}; 10 mice per group ($n = 10$); after 1, 4, and 6 h post-infection. Results were considered highly significant (****) when P value < 0.0001. P value was calculated using a 95% class interval and paired t-test.

In conclusion, our study presents SMJ-2 as a promising solution to antibiotic resistance. Unlike natural antibiotics, SMJ-2, a chemically synthesized compound, effectively targets drug-resistant gram-positive bacteria like MRSA and VRE. Its unique mechanism disrupts bacterial metabolism, offering a novel approach to combat multidrug resistance. With favorable properties and efficacy in diverse infection models, SMJ-2 shows potential for clinical use. This highlights the transformative role of chemical synthesis in addressing antibiotic-resistant pathogens.

Materials and methods

General Chemistry

Described in detail in the supplementary methodology.

Table 2 | Biochemical test from blood serum of drug-treated mice at various concentrations

Stage 2 (SMJ-2)		
Investigation	**Mice [500 mg/kg; (*n* = 3)]**	**Mice [Vehicle control; (*n* = 3)]**
Body weight (Before dosing) (gm)	18.3 ± 0.62	17.6 ± 0.15
Body weight (After dosing) (gm)	17.48 ± 0.75	17.36 ± 1.44
Blood Glucose (After dosing) (mg/dL)	236 ± 33.04	280 ± 29.36
Triglycerides	65.66 ± 7.76	75 ± 10.53
Renal Function test complete (Kidney Panel)		
Calcium	8.5 ± 0.26	8.6 ± 0.26
Alkaline Phosphatase (ALP)	123.66 ± 16.56	107 ± 9.84
Phosphorous (Serum)	8.03 ± 1.01	8 ± 1.45
Blood urea	43.17 ± 4.3	34.66 ± 2.3
Serum Creatinine	0.26 ± 0.005	0.25 ± 0.01
Uric acid	1.66 ± 0.208	1.8 ± 0.5
Liver Function Test with GGTP		
Bilirubin; Indirect (Unconjugated)	0.136 ± 0.020	0.13 ± 0.026
Bilirubin; Direct (Conjugated)	0.1 ± 1.7E-17	0.1 ± 1.7E-17
Bilirubin (Total)	0.236 ± 0.020	0.23 ± 0.026
Serum glutamic oxaloacetic transaminase (SGOT)/aspartate aminotransferase (AST)	79.66 ± 7.76	57.33 ± 5.68
Serum glutamic pyruvic transaminase (SGPT)/alanine aminotransferase (ALT)	31.66 ± 6.42	21.33 ± 2.88
Alkaline Phosphatase	123.66 ± 16.56	107 ± 9.84
Total Proteins	4.9 ± 0.3	4.7 ± 0.36
Albumin	2.8 ± 0.1	2.76 ± 0.05
Globulin	2.1 ± 0.2	1.93 ± 0.32
A/G ratio	1.33 ± 0.05	1.46 ± 0.23

General procedure for the synthesis of SMJ-2 and SMJ-4

Described in detail in the supplementary methodology.

Bacterial strains, cell lines, and growth medium

In the current investigation, *S. aureus* ATCC MSSA 29213, ATCC MRSA 43300, ATCC MRSA 33591, ATCC BAA 1717, ATCC BAA 39, *Enterococcus faecium* ATCC 51559, ATCC 19434, *Enterococcus faecalis* ATCC 29212, ATCC 51299 and *B. subtilis* MTCC 121 and clinical isolates of *S. aureus* were employed. Cation-adjusted BBLTM Mueller Hinton II Broth (CA-MHB), Mueller-Hinton agar (MHA), and tryptic soya broth were used in all bacterial media. DMEM (ThermoFisher) and FBS (ThermoFisher) were employed for cell culture research. Human Embryonic Kidney Cells (HEK-293), hepatoblastoma cell line (HepG2), and human leukemia macrophage cells (THP-1) were used for ex vivo experiments. THP-1 cells were induced by phorbol 12-myristate 13-acetate at 20 ng/mL and incubated for 24 h to convert to macrophages.

Broth microdilution assay

The CLSI standards[36] were used to establish the minimum inhibitory concentration (MIC) using broth microdilution. The experiment was conducted on 96-well round-bottom plates with a total reaction volume of 200 µL. The drugs were prepared in two-fold serial dilutions. The bacterial suspension OD_{600nm} was adjusted to 0.25–0.3, and it was diluted such that each well ultimately contained 5×10^5 CFU mL^{-1}. For 18 h, the plates were incubated at 37 °C.

Time-kill kinetics

As a suspension, *S. aureus* ATCC 43300 and ATCC 29213 were cultivated until the mid-exponential phase; OD_{600nm} was then adjusted to 0.3. The bacteria were challenged with vancomycin, linezolid, oxacillin, SMJ-2, and SMJ-4 at 10 × MIC. At various time intervals (0, 2, 4, 8, 24 h), the culture was assessed for the bacterial count and expressed as CFU mL^{-1}[17, 37]. For the stationary phase time-kill kinetic study, *S. aureus* ATCC 43300 and ATCC 29213 cells from a similar overnight culture were diluted 10 × times in PBS and then treated with vancomycin, linezolid, oxacillin, SMJ-2, and SMJ-4 at 10 × MIC in culture tubes at 37 °C and 225 rpm. The culture's bacterial count was assessed and expressed as CFU mL^{-1} at different intervals (0, 2, 4, 8, 24 h).

Persisters assay

The experiment was carried out mainly as described with minor adjustments[38]. Stationary phase *S. aureus* ATCC 29213 cells (from a 24 h old culture) were diluted 10 × times and then treated with 10 × MIC of oxacillin in TSB medium for 24 h at 37 °C under shaking conditions to form antibiotic-induced persister cells. Aliquots were withdrawn regularly to determine the number of viable bacteria that survived oxacillin exposure. To treat persisters with our compounds and comparative antibiotics, oxacillin-exposed cultures were centrifuged after 14 h of treatment and washed thrice with 1 × PBS to remove any added drug traces. Isolated persisters were resuspended in 1 × PBS. SMJ-2 was added at different concentrations to each 1000 µL aliquot of persister cells at indicated concentrations, followed by incubation at 37 °C for 24 h at 200 rpm. DMSO was used as vehicle control. The viable colonies were determined after 24 h of incubation and represented as $\log_{10}$ CFU mL^{-1}. A time-dependent kinetics assay to study the rate of killing of persisters by SMJ-2 (5×, 10×, 20 × MIC) was performed simultaneously by withdrawing aliquots at regular intervals to determine the viable cell count.

Resistance studies

S. aureus ATCC 29213, ATCC 43300, and *B. subtilis* MTCC 121 cells were used for sequential resistance development. Cells were grown to the mid-log phase, and the experiment was done as described earlier[37, 39]. OD_{600nm} was adjusted to 0.3, which was further diluted 10 × times, containing a sub-inhibitory concentration of SMJ-2. After that, the cells were exposed to a sub-inhibitory concentration at 37 °C and passaged every 24 h. MIC was determined every day using broth micro-dilution assay. The experiment was performed in duplicates and two biological replicates.

DiOC2(3) assay

Using the membrane potential-sensitive fluorescent dye DiOC2(3), the depolarization of *S. aureus* ATCC 29213's plasma membrane potential was measured as previously described with some modifications[40]. *S. aureus* was cultivated in MHB until it reached the mid-exponential phase, washed with PBS, and then resuspended in a resuspension buffer (130 mM NaCl, 60 mM Na_2HPO_4, 60 mM NaH_2PO_4, 10 mM glucose, 5 mM KCl, and 0.5 mM $MgCl_2$)[41]. The pH of the resuspension buffer was adjusted to 7 using NaOH, and OD_{600nm} was adjusted to 1. Following a 15-minute incubation at 37 °C, the bacteria were treated with 30 µM DiOC2(3) under the same circumstances. Bacteria were transferred to 96-well plates with 190 µL per well after the incubation period, and 20 µL of SMJ-2 and SMJ-4 treatments at varying concentrations were administered (4, 8, 16, and 32 MIC). The positive control used was CCCP. A hybrid plate reader was used to monitor the fluorescence change at 450/670 nm following a 5-minute incubation of the compound and dye at room temperature.

DiSC3(5) assay

S. aureus ATCC 29213 was cultivated to mid-exponential phase at 37 °C. The cells were centrifuged, washed three times at 4000 × *g* for 10 min, and resuspended and diluted in 50 mM HEPES buffer and 0.1% glucose to attain an OD_{600nm} of 0.1. DiSC3(5) dye (Sigma Aldrich) at 1 µM concentration

and 300 mM KCl (to counteract the outer and cytoplasmic K+ concentrations) in HEPES buffer were added to the cells and incubated in the dark for 10 min at room temperature to stabilize the probe fluorescence[42–45]. SMJ-2 and SMJ-4 were added to the cells at 1×, 2×, and 4 × MIC, and nigericin and valinomycin (Sigma–Aldrich) were employed as a positive control for 5 min. The fluorescence leakage was then measured at a $\lambda_{excitation}$/ $\lambda_{emission}$ of 622/670 nm.

Membrane permeability assay

The membrane permeabilization assay measured the fluorescence of propidium iodide (PI) penetrating the membrane according to the Invitrogen™ Propidium Iodide kit (Thermo Fisher Scientific) protocol with certain modifications. In CA-MHB, *S. aureus* ATCC 29213 was incubated and allowed to grow up to the mid-exponential stage with an OD_{600nm} of 0.3. The 500 µL bacterial suspension was treated with SMJ-2, SMJ-4, at 1×, 2×, 4×, and 10 × MIC and paenibacillin (20 µM) for 30 min. After treatment, bacterial cell OD_{600nm} was normalized, and then the culture was washed thrice with normal saline (0.85% NaCl) and suspended in PBS. The suspensions were treated with 30 µM PI and incubated at room temperature for 15–20 min. Any unbound PI was eliminated by centrifuging the suspensions at 13,000 × *g* for 5 min and then suspended in 500 µL PBS. 100 µL suspensions were dispensed in a 96-well plate, and fluorescence was measured at a $\lambda_{excitation}$/ $\lambda_{emission}$ of 490 and 635 nm, respectively, after 30 min.

Determination of intracellular ATP Levels. The experiment was performed using the Promega BacTiter-Glo™ Microbial Cell Viability Assay kit according to the manufacturer's guidelines. *S. aureus* ATCC 29213 strain was grown in MHB at 37°C till the mid-exponential phase. SMJ-2 and SMJ-4 treated culture (10^5 cells mL^{-1}) at varying concentrations (1/2×, 1×, 5×, and 10 × MIC) were incubated for 5 h at 37 °C. CCCP was used as a positive control at 1 × MIC (0.5 µg mL^{-1}). After incubation, OD_{600nm} of all treated and untreated culture groups was normalized (Supplementary Fig. 12). 100 µL of cells were moved to a 96-well black plate, and an equal volume of BacTiter-Glo™ Reagent was added in each well. The plate was kept on an orbital shaker for five minutes, and luminescence was measured using a Synergy HT multi-mode microplate reader. All steps are performed at room temperature (22–25 °C). An 0.25–1 s integration time per well should be a guideline.

Extraction of total RNA and RNA sequencing

Overnight grown *S. aureus* 29213 was treated with SMJ-2 and SMJ-4 (1 × MIC) for 16 h after diluting 100 × times. The culture was treated with 5 M guanidine thiocyanate (GTC) for 5 minutes after being centrifuged at 10,000 × *g*. Afterward, it was centrifuged, pelleted, and kept at −80 °C until RNA isolation. The pellet was then washed with DEPC water, resuspended in 1 mL of TRIzol reagent (Thermo Fisher Scientific, Inc.), and lysed using bead beating for 30 s at 3–5 min, three times at a speed of 6 rpm. After each cycle, the suspension was immediately put on hold. Following the manufacturer's instructions, RNA was isolated from the bacterial suspension using the Qiagen RNeasy Mini kit.

Bioinformatic steps

Read quality check. From the fastq file, we examined the distributions of the following parameters: Base quality score, Sequence quality score, Average base content per Read, GC distribution in Reads, PCR amplification problem, overrepresented sequence check, and Adapter trimming. Where appropriate, we shortened sequence reads to preserve high-quality sequences for subsequent analysis based on the quality assessment of the fastq files. Furthermore, the research did not include any of the poor-quality sequence reads. Utilizing Trimmomatic (v-0.36), the adapter was trimmed.

Removal of contamination. Assuming that poly-A-tailed RNAs were sequenced, we eliminated the undesirable sequences from the sample for the RNA-Sequencing analysis, particularly non-poly-A-tailed RNAs. Ribosomal RNAs, transfer RNAs, adaptor sequences, and other sequences were among the undesirable ones. Bowtie2 (2.2.4) was used to remove contamination. Read alignment: To the reference *S. aureus* genome, the paired-end reads have been aligned (https://ftp.ncbi.nlm.nih.gov/genomes/all/GCF/000/013/425/GCF_000013425.1_ASM1342v1/GCF_000013425.1_ASM1342v1_genomic.fna.gz). Alignment was performed using HISAT2 (2.1.0).

Estimating gene expression. The estimated gene expression is based on the aligned readings. FeatureCount (1.5.2) was used to estimate the raw read counts. DESeq2 was used to normalize read count data.

Analysis of differential expression. DESeq2 was used to normalize the raw read counts. The fold change was calculated as the ratio of normalized read counts for treated versus control samples. The *p*-value (<=0.05) was used as the initial gene filter. It was discovered that these log2 (fold change) values were normally distributed. Genes found to have a fold change of $-1 <= \log2 >= 1$ were deemed statistically significant.

GO annotation and pathway analysis. The Panther database performed GO annotation and Reactome pathway information for differentially expressed genes. The BioProject ID is PRJNA976500 is linked below https://submit.ncbi.nlm.nih.gov/subs/bioproject/SUB13473442/overview.

RT-PCR. Thermo Fisher Scientific, Inc.'s SuperScriptTM III PlatinumTM One-Step qRT-PCR Kit was used to create cDNA following the manufacturer's instructions for the reverse transcription polymerase chain reaction. The PCR thermocycling conditions were as follows: 50 °C for 14.02 min, 95 °C for 2 min, 40 cycles of 95 °C for 15 s and 60 °C for 30 s, and a melt curve of 95 °C for 15 seconds and 60 °C for 1 min. Relative gene expression was determined using the power $2^{-\Delta\Delta CT}$ method. The housekeeping gene 16 s rRNA was used as an endogenous control to normalize the expression levels of target genes. Each sample was evaluated in duplicate, and all samples were examined parallel for their expression. The average values from the replicates were used to calculate the fold induction. The primer sequence is depicted in Supplementary Table 7.

Effect of SMJ-2 and SMJ-4 on the cellular bioenergetic state (NADH/H +). *S. aureus* ATCC 29213 was grown to the mid-log phase, and the experiment was performed as described earlier[18]. The cells were rinsed and resuspended in 1 × PBS with 2 µM resazurin (Sigma–Aldrich, USA), a respiration indicator dye, and 0.4% w/v glucose as the primary carbon source. After being treated with SMJ-2, SMJ-4, and polymyxin B[18] at ½×, 1×, and 2 × MIC, the cell suspension (OD_{600nm} 0.25) was kept for 3 h at 37 °C. MIC of polymyxin B is 32 µg mL^{-1} on *S. aureus* ATCC 29213. At 530 nm excitation and 590 nm emission, the fluorescence of resazurin's reduced product was detected and was used to determine NADH/H+ levels. OD_{600nm} was normalized, and fluorescence was measured.

Iodonitrotetrazolium reduction assay. With certain adjustments, the experiment was carried out as previously described[24]. *S. aureus* cells were grown to the mid-exponential phase, and OD_{600nm} was adjusted to 0.25. The bacterial culture was treated with SMJ-2 and SMJ-4 at 1×, 5×, and 10 × MIC. Each treatment was kept for 5 h at 37 °C and 200 RPM in a volume of 1 mL. After incubation, OD_{600nm} in all treated and untreated culture groups was normalized (Supplementary Fig. 12), and the cells were centrifuged. Media was removed, the pellet was washed with potassium phosphate buffer twice, and finally resuspended in 400 µL potassium phosphate buffer containing 0.5 mg mL^{-1} of INT, a known electron acceptor. Cells were moved to a transparent, 96-well plate with a flat bottom after incubation at 30 °C in the dark for 45 min. CCCP was used as a positive control. At 490 nm, absorbance was also measured.

Staphyloxanthin extraction and spectrometric measurement of its biosynthetic intermediates. *S. aureus* ATCC 29213 was grown for 48 h and then diluted 100 × times in CA-MHB. To extract carotenoid pigments, 5 mL bacterial culture was grown in the absence and presence of SMJ-2 and SMJ-4 at sub-inhibitory concentrations (0.75 × MIC, 0.5 × MIC, 0.25 × MIC) for 24 h and were centrifuged at 8000 rpm for 10 min. PBS was used to rinse the cell pellets before they were suspended in 500 µL of methanol. The tubes were shaken for 5 h at 400 rpm and 55 °C while covered in aluminum foil. The extracted pigments were then separated from the supernatant by centrifuging the tubes. A plate reader was used to measure the absorbance of staphyloxanthin at 462 nm.

The staphyloxanthin intermediates in the collected supernatant were quantified using a plate reader and various wavelengths. The absorbance wavelengths used were 286 nm for 4,4′ -diapophytoene, 435 nm for 4,4′ -diaponeurosporene, 455 nm for 4,4′ -diaponeurosporenic acid. The control was methanol[46, 47].

Measurement of ROS production. As previously mentioned[47], 2,7-dichlorofluorescein diacetate (DCFH2-DA) (Sigma-Aldrich, India) was used as a fluorescent probe to evaluate ROS production. Overnight bacterial culture was diluted to an OD_{600nm} of ≈ 0.1. Then, the culture was treated with 0.5 × MIC of SMJ-2, SMJ-4, and the positive control miconazole for 5 h, untreated bacterial culture was used as control. Briefly, SMJ-2, SMJ-4, miconazole treated, and untreated cell suspensions were pelleted and washed three times with PBS, and the final OD was normalized equally. Then, the samples were supplemented with 5 µM DCFH2-DA and incubated at 37 °C in the dark for half an hour. The fluorescence was measured at 485/530 nm using a Synergy HT multi-mode microplate after half an hour of incubation.

H_2O_2 sensitivity assay. *S. aureus* ATCC 29213 strain was cultured for 48 h in TSB. Then, the culture was diluted 200 × times, and the cells were treated with 0.5× and 0.75 × MIC of SMJ-2, SMJ-4, and miconazole each, and one tube was kept untreated. These tubes were then incubated at 37 °C for 5 h. The OD_{600nm} was normalized, then the treated and untreated cultures were spread on plates. 20 µL of 1.5% H_2O_2 was placed in the center. The plates were incubated at 37 °C for 24 h. The zone of inhibition was measured, and the photograph was captured.

Mouse virulence subcutaneous skin infection model. The experiment was carried out as described with a few modifications[48, 49]. Four groups, each with six mice, were created from 6 to 8-week-old female BALB/c mice. With the aid of a trimmer, the dorsal hairs were removed. Veet was applied for five minutes to remove any remaining hair before being cleaned with ethanol. After that, sandpaper was used to make a wound on the skin until the epidermis was scraped off but did not bleed. As previously mentioned, bacterial preparation was carried out with *S. aureus* ATCC 29213 cultured in the absence and presence of SMJ-2 and miconazole at 0.75 × MIC, respectively. A 10 µL volume of the bacterial culture was then administered to the injured area of the respective groups after being washed in PBS, centrifuged, and adjusted to an OD_{600nm} of 1. After 24 h, one control group was sacrificed, and the remaining group was sacrificed after 96 h through cervical dislocation. From the affected area, the skin was cut off and collected. The positive control in this study was miconazole[26]. Infection was determined in $\log_{10}$ CFU/gm of skin based on the weight of the cut skin and the infection rate per gram of skin.

Crystal violet biofilm inhibition. The experiment was performed with some modifications[50]. *S. aureus* was cultured overnight in Soyabean Casein Digest Medium (Tryptone Soya Broth) (HIMEDIA) with 2.5% glucose for biofilm formation. In microtitre plates containing SMJ-2 and SMJ-4, the culture was diluted 200 × times. After 48 h at 37 °C, the wells were washed twice with PBS to remove the planktonic cells, then fixated with methanol for 15 min and air-dried at 37 °C in an inverted position for 10 min. The cells in the dried wells were stained with 0.05% (w/v) crystal violet and incubated at room temperature for 10 min. The cells were washed in PBS until the medium-containing control wells (wells without bacterial biofilm, negative control) became colorless. Finally, 200 µL of ethanol: acetone (80:20) combination was added to the wells and incubated at room temperature for 10 min. A Synergy HT multi-mode microplate reader was used to detect absorbance at 570 nm.

Crystal violet biofilm eradication. *S. aureus* was cultured overnight in Soyabean Casein Digest Medium (Tryptone Soya Broth) (HIMEDIA) with 2.5% glucose to form biofilms. After that, the culture was diluted 200 × times. The plates were left to incubate for 48 h. The biofilm was washed with PBS twice to remove planktonic cells. Then 200 µL of TSB containing SMJ-2 and SMJ-4 were introduced to eradicate the pre-formed biofilm during the maturation stage (48 h biofilms) (2.5% glucose). As a control, untreated biofilms were used. At 37 °C, the plates were kept in the incubator for 24 h. The next day, non-adherent cells were removed from each well, and the adhering biofilm was rinsed twice with PBS before being fixated with methanol for 15 min and air-drying at 37 °C in an inverted position for 10 min. The biofilm was evaluated using CV, and biofilm eradication was calculated as described. The cells in the dry wells were stained with 0.05% (w/v) CV and incubated at room temperature for 10 min. The cells were washed in PBS until the medium containing control wells became colorless. Finally, 200 µL of ethanol: acetone (80:20) combination was added to the wells and incubated at room temperature for 10 min. A Synergy HT multi-mode microplate reader was used to detect absorbance at 570 nm[50].

Identifying viable cell populations in biofilms. The MTT test was also used to determine the living cells in the biofilm. The experiment was carried out identically as described previously, except that instead of a CV, MTT (500 µg mL^{-1} final concentration) was used. After washing the cells, MTT was added, and the plates were kept for 4 h at 37 °C. MTT was dissolved in a solubilizing solution. At 4.7 pH, the formazan crystals were solubilized in a 100 µL stopping solution comprising 40% (vol/vol) dimethylfo^{4}rmamide (DMF) in 2% (vol/vol) glacial acetic acid and 16% (wt/vol) sodium dodecyl sulfate (SDS). At 570 nm, the absorbance was measured. The results show the % inhibition of live adherent bacteria in the biofilm compared to the control (untreated biofilm)[51].

Confocal microscopy. The nucleic acids of the biofilm cells were stained with SYTO9 dye (Invitrogen, Life Technologies, USA) and seen using confocal laser scanning microscopy (CLSM), according to protocol[50]. CLSM was utilized to confirm the efficacy of SMJ-2 at 4× and 8 × MIC to visualize the effect on sterile 18 mm glass coverslips coated in poly-L lysine and set in a 12-well polystyrene plate (Falcon). *S. aureus* 839 was used to prepare the biofilm. The plate was then kept in an incubator for 24 h at 37 °C. The plates were rinsed with regular saline to get rid of planktonic cells. After being diluted 1000 × times in PBS, SYTO9 was added and left to rest at room temperature for 20–30 min in the biofilm wells. Following incubation, three further saline washes were administered, and using a Nikon A1 plus Ti confocal microscope equipped with a Nikon A1R scan head, pictures were viewed on an oil immersion lens (40X). NIS Elements software was used to take the pictures.

Post-antibiotic assay. Described in detail in the supplementary methodology.

Physicochemical, lipophilicity, and pharmacokinetic properties of compounds. Described in detail in the supplementary methodology.

Hemolysis assay. Described in detail in the supplementary methodology.

Mammalian cytotoxicity. Described in detail in the supplementary methodology.

Acute toxicity, blood-biochemical, and histopathological studies in animal model. The experiment was carried out mainly as described with minor adjustments[29]. There were two stages to this experiment. The result of each stage determined the following one (i.e., whether to halt or continue to the next level). Stage 1 consisted of three groups, with three mice in each group. Doses were administered as follows: 20 mg kg^{-1} (stage 1, group 1), 40 mg kg^{-1} (stage 1, group 2), 80 mg kg^{-1} (stage 1, group 3). Stage 2 involved three groups, again comprising three mice in each group: 100 mg kg^{-1} (stage 2, group 1), 250 mg kg^{-1} (stage 2, group 2), 500 mg kg^{-1} (stage 2, group 3) (Supplementary Table 10). Animals were monitored for 7 days after administration, and mice were monitored every 2 h on the first day and every 12 h for the remaining days. Both fatalities and behavioral toxicity symptoms were noted. After 7 days, mice received intraperitoneal injections of xylazine (10 mg kg^{-1}) and ketamine (90 mg kg^{-1})[52]. After that, a small amount of blood was drawn from the mouse's tail vein to measure its blood glucose level. The retro-orbital method collected 500–600 µL of blood from mice. The blood in MCT was centrifuged for 10 min at 1000 × *g* after being left at room temperature undisturbed for 30 min. Then, serum was gathered and stored in a refrigerator at −80 °C. The vital body organs—lung, heart, brain, liver, kidney, and spleen- were removed from the mice after being dissected and preserved in formalin solution with 10% neutral buffered formaldehyde. The blood-biochemical and histopathological studies were outsourced from a private medicos center.

In vivo thigh infection model. The experiment was carried out mainly as described with minor adjustments[37, 50]. To induce neutropenia, two intraperitoneal doses of cyclophosphamide at 150 and 100 mg kg^{-1} each were given to female BALB/c mice four and one day before infection, respectively. There were four groups and each group contains six mice ($n = 6$). The mice were then given an intramuscular injection of 50 µL of *S. aureus* ATCC 43300 (2.5×10^7 CFU mL^{-1}) in the right thigh. 20 mg kg^{-1} of SMJ-2 and 20 mg kg^{-1} of linezolid (Cayman Chemical Company) were given orally to mice 4 h after infection. After 4 h, cervical dislocation was used to sacrifice one group of infected mice. CFUs were identified after the right thighs were removed and homogenized. After administering the dose of SMJ-2 and linezolid injections, the other three mice groups were sacrificed by cervical dislocation 20 h later. Each of the groups' CFU from the right thigh was counted.

Mouse peritonitis model. With a few modifications, the experiment was conducted as previously described[37,53]. 500 µL of a suspension of *S. aureus* ATCC 43,300 at a concentration of 2×10^9 CFU mL^{-1} was administered intraperitoneally to the mice. 20 mg kg^{-1} of SMJ-2 and 20 mg kg^{-1} of linezolid were subcutaneously administered to all groups ($n = 10$) at 1, 3, and 5 h following infection. For seven days, mice's weight variations and survival conditions were observed. The cervical dislocation method was used to sacrifice the mice that had lasted until the seventh day.

Statistical analyses. Statistical analyses were performed using GraphPad Prism software for Windows (version 8.0.2; GraphPad Software, Inc., San Diego, CA). The information is shown as mean and standard deviation. Paired *t*-tests (two-tailed) were employed to find group differences. *P* values of 0.05 (*) were regarded as statistically significant; 0.01 (**), 0.001 (***), and 0.0001 (****) were considered highly significant.

Reporting summary

Further information on research design is available in the Nature Portfolio Reporting Summary linked to this article.

Data availability

The BioProject ID is PRJNA976500 is linked below https://submit.ncbi.nlm.nih.gov/subs/bioproject/SUB13473442/overview. Data supporting the findings in this article are available within the article and supplementary information, and available from the corresponding author upon reasonable request. All the numerical source data underlying the graphs presented in the main figures are provided as Supplementary Data 1 and Supplementary Data 2.

Received: 12 February 2024; Accepted: 1 October 2024;
Published online: 12 November 2024

References

1. Lewis, K. The science of antibiotic discovery. *Cell* **181**, 29–45 (2020).
2. Wertheim, H. F. et al. Risk and outcome of nosocomial Staphylococcus aureus bacteraemia in nasal carriers versus non-carriers. *Lancet* **364**, 703–705 (2004).
3. Kehl-Fie, T. E. et al. MntABC and MntH contribute to systemic Staphylococcus aureus infection by competing with calprotectin for nutrient manganese. *Infect. Immun.* **81**, 3395–3405 (2013).
4. CDC. Antibiotic Resistance Threats in the United States, 2019. Atlanta, GA:U.S. Department of Health and Human Services, CDC https://doi.org/10.15620/cdc:82532 (2019).
5. Doernberg, S. B. et al. Gram-positive bacterial infections: research priorities, accomplishments, and future directions of the antibacterial resistance leadership group. *Clin. Infect. Dis.* **64**, S24–S29 (2017).
6. Ni, S. et al. Novel staphyloxanthin inhibitors with improved potency against multidrug resistant staphylococcus aureus. *ACS Med. Chem. Lett.* **9**, 233–237 (2018).
7. Chandal, N. et al. Efflux pump inhibitory potential of indole derivatives as an arsenal against norA over-expressing Staphylococcus aureus. *Microbiol. Spectr.* **11**, e04876-04822 (2023).
8. Paiva, C. N. & Bozza, M. T. Are reactive oxygen species always detrimental to pathogens? *Antioxid. Redox Signal.* **20**, 1000–1037 (2014).
9. Schurig-Briccio, L. A., Yano, T., Rubin, H. & Gennis, R. B. Characterization of the type 2 NADH:menaquinone oxidoreductases from Staphylococcus aureus and the bactericidal action of phenothiazines. *Biochim. Biophys. Acta* **1837**, 954–963 (2014).
10. Mohapatra, S. S., Dwibedy, S. K. & Padhy, I. Polymyxins, the last-resort antibiotics: mode of action, resistance emergence, and potential solutions. *J. Biosci.* **46**, https://doi.org/10.1007/s12038-021-00209-8 (2021).
11. Stokes, J. M. et al. A deep learning approach to antibiotic discovery. *Cell* **180**, 688–702.e613 (2020).
12. Zhao, X. & Kuipers, O. P. Brevicidine B. A new member of the brevicidine family, displays an extended target specificity. *Front. Microbiol.* **12**, https://doi.org/10.3389/fmicb.2021.693117 (2021).
13. Miller, C. et al. PanG, a new ketopantoate reductase involved in pantothenate synthesis. *J. Bacteriol.* **195**, https://doi.org/10.1128/JB.01740-12 (2012).
14. Leonardi, R. et al. A pantothenate kinase from staphylococcus aureus refractory to feedback regulation by coenzyme A*. *J. Biol. Chem.* **280**, 3314–3322 (2005).
15. Kwong, W. K., Zheng, H. & Moran, N. A. Convergent evolution of a modified, acetate-driven TCA cycle in bacteria. *Nat. Microbiol.* **2**, 17067 (2017).
16. Heikal, A. et al. Structure of the bacterial type II NADH dehydrogenase: a monotopic membrane protein with an essential role in energy generation. *Mol. Microbiol.* **91**, 950–964 (2014).
17. Schurig-Briccio, L. A. et al. Role of respiratory NADH oxidation in the regulation of Staphylococcus aureus virulence. *EMBO Rep.* **21**, e45832 (2020).
18. Saini, M. et al. Small molecule IITR00693 (2-Aminoperimidine) synergizes polymyxin B activity against staphylococcus aureus and pseudomonas aeruginosa. *ACS Infect. Dis.* **9**, 692–705 (2023).
19. Deris, Z. Z. et al. A secondary mode of action of polymyxins against Gram-negative bacteria involves the inhibition of NADH-quinone oxidoreductase activity. *J. Antibiot.* **67**, 147–151 (2014).

20. Petri, J. et al. Structure of the NDH-2 - HQNO inhibited complex provides molecular insight into quinone-binding site inhibitors. *Biochim. Biophys. Acta Bioenerg.* **1859**, 482–490 (2018).
21. Bender, D. A. in *Encyclopedia of Food Sciences and Nutrition (Second Edition)* (ed Benjamin Caballero) 5851–5856 (Academic Press, 2003).
22. Yuan, W. et al. Indole-core-based novel antibacterial agent targeting FtsZ. *Infect. Drug Resist* **12**, 2283–2296 (2019).
23. Korge, P., Calmettes, G. & Weiss, J. N. Reactive oxygen species production in cardiac mitochondria after complex I inhibition: modulation by substrate-dependent regulation of the NADH/NAD(+) ratio. *Free Radic. Biol. Med.* **96**, 22–33 (2016).
24. Farha, MayaA., Verschoor, ChrisP., Bowdish, D. & Brown, EricD. Collapsing the proton motive force to identify synergistic combinations against staphylococcus aureus. *Chem. Biol.* **20**, 1168–1178 (2013).
25. El-Ganiny, A. M., Gad, A. I., El-Sayed, M. A., Shaldam, M. A. & Abbas, H. A. The promising anti-virulence activity of candesartan, domperidone, and miconazole on Staphylococcus aureus. *Braz. J. Microbiol.* **53**, 1–18 (2022).
26. Elmesseri, R. A., Saleh, S. E., Elsherif, H. M., Yahia, I. S. & Aboshanab, K. M. Staphyloxanthin as a potential novel target for deciphering promising anti-staphylococcus aureus agents. *Antibiotics* **11**, https://doi.org/10.3390/antibiotics11030298 (2022).
27. Subhadra, B., Kim, D. H., Woo, K., Surendran, S. & Choi, C. H. Control of biofilm formation in healthcare: recent advances exploiting quorum-sensing interference strategies and multidrug efflux pump inhibitors. *Materials* **11**, https://doi.org/10.3390/ma11091676 (2018).
28. Kikuchi, K. & Shimizu, K. Post-antibiotic effect and clinical significance. *Nihon Rinsho. Jpn. J. Clin. Med.* **50**, 1165–1172 (1992).
29. Chinedu, E., Arome, D. & Ameh, F. S. A new method for determining acute toxicity in animal models. *Toxicol. Int.* **20**, 224–226, (2013).
30. Walum, E. Acute oral toxicity. *Environ. Health Perspect.* **106**, 497–503 (1998).
31. Ahmed, M. H. et al. Methicillin-resistant Staphylococcus aureus, vancomycin-resistant Enterococcus faecalis and Enterococcus faecium active dimeric isobutyrylphloroglucinol from Ivesia gordonii. *Nat. Prod. Commun.* **9**, 221–224 (2014).
32. Kaplan, N. et al. Mode of action, in vitro activity, and in vivo efficacy of AFN-1252, a selective antistaphylococcal FabI inhibitor. *Antimicrbial Agents and Chemotherapy* **56**, 5865–5874 (2012).
33. Taylor, S. D. & Palmer, M. The action mechanism of daptomycin. *Bioorg. Med. Chem.* **24**, 6253–6268 (2016).
34. Spry, C., Kirk, K. & Saliba, K. J. Coenzyme A biosynthesis: an antimicrobial drug target. *FEMS Microbiol. Rev.* **32**, 56–106 (2008).
35. Matsumoto, Y. et al. A critical role of mevalonate for peptidoglycan synthesis in Staphylococcus aureus. *Sci. Rep.* **6**, 22894 (2016).
36. Humphries, R., Bobenchik, A. M., Hindler, J. A. & Schuetz, A. N. Overview of changes to the clinical and laboratory standards institute performance standards for antimicrobial susceptibility testing, M100, 31st Edition. *J. Clin. Microbiol* **59**, e00213–e00221 (2021).
37. Ling, L. L. et al. A new antibiotic kills pathogens without detectable resistance. *Nature* **517**, 455–459 (2015).
38. Bhando, T. et al. Antibacterial properties and in vivo efficacy of a novel nitrofuran, IITR06144, against MDR pathogens. *J. Antimicrob. Chemother.* **75**, 418–428 (2019). J Journal of Antimicrobial Chemotherapy.
39. Bogdanovich, T., Ednie, L. M., Shapiro, S. & Appelbaum, P. C. Antistaphylococcal activity of ceftobiprole, a new broad-spectrum cephalosporin. *Antimicrob. Agents Chemother.* **49**, 4210–4219 (2005).
40. Sovari, S. N. et al. Design, synthesis and in vivo evaluation of 3-arylcoumarin derivatives of rhenium(I) tricarbonyl complexes as potent antibacterial agents against methicillin-resistant Staphylococcus aureus (MRSA). *Eur. J. Med. Chem.* **205**, 112533 (2020).
41. Hudson, M. A., Siegele, D. A. & Lockless, S. W. Use of a fluorescence-based assay to measure escherichia coli membrane potential changes in high throughput. *Antimicrob. Agents Chemother.* **64**, https://doi.org/10.1128/aac.00910-20 (2020).
42. Wu, M., Maier, E., Benz, R. & Hancock, R. E. Mechanism of interaction of different classes of cationic antimicrobial peptides with planar bilayers and with the cytoplasmic membrane of Escherichia coli. *Biochemistry* **38**, 7235–7242 (1999).
43. Morin, N. et al. Mechanism of bactericidal activity of microcin L in Escherichia coli and Salmonella enterica. *Antimicrob. Agents Chemother.* **55**, 997–1007 (2011).
44. Cheng, M., Huang, J. X., Ramu, S., Butler, M. S. & Cooper, M. A. Ramoplanin at bactericidal concentrations induces bacterial membrane depolarization in Staphylococcus aureus. *Antimicrob. Agents Chemother.* **58**, 6819–6827 (2014).
45. French, S. et al. Potentiation of antibiotics against gram-negative bacteria by Polymyxin B analogue SPR741 from unique perturbation of the outer membrane. *ACS Infect. Dis.* **6**, 1405–1412 (2020).
46. Leejae, S., Hasap, L. & Voravuthikunchai, S. P. Inhibition of staphyloxanthin biosynthesis in Staphylococcus aureus by rhodomyrtone, a novel antibiotic candidate. *J. Med. Microbiol.* **62**, 421–428 (2013).
47. Valliammai, A. et al. Staphyloxanthin inhibitory potential of thymol impairs antioxidant fitness, enhances neutrophil mediated killing and alters membrane fluidity of methicillin resistant Staphylococcus aureus. *Biomed. Pharmacother.* **141**, 111933 (2021).
48. Tong, S. Y. et al. Virulence of endemic nonpigmented northern Australian Staphylococcus aureus clone (clonal complex 75, S. argenteus) is not augmented by staphyloxanthin. *J. Infect. Dis.* **208**, 520–527 (2013).
49. Liu, G. Y. et al. Staphylococcus aureus golden pigment impairs neutrophil killing and promotes virulence through its antioxidant activity. *J. Exp. Med.* **202**, 209–215 (2005).
50. Blaskovich, M. A. T. et al. The antimicrobial potential of cannabidiol. *Commun. Biol.* **4**, 7 (2021).
51. Trafny, E. A., Lewandowski, R., Zawistowska-Marciniak, I. & Stępińska, M. Use of MTT assay for determination of the biofilm formation capacity of microorganisms in metalworking fluids. *World J. Microbiol. Biotechnol.* **29**, 1635–1643 (2013).
52. Levin-Arama, M. et al. Subcutaneous compared with intraperitoneal KetamineXylazine for anesthesia of mice. *J. Am. Assoc. Lab. Anim. Sci.* **55**, 794–800 (2016).
53. Gao, P. et al. Antivirulence Agent as an Adjuvant of β-Lactam Antibiotics in Treating Staphylococcal Infections. *Antibiotics (Basel, Switzerland)*. **11**, 819 (2022).

Acknowledgements

We thank the director of CSIR-IMTECH for providing the necessary facilities and infrastructure to complete this work. NC expresses gratitude to the Indian Council of Scientific and Industrial Research (CSIR) for the senior research scholarship. The clinical isolates utilized in this investigation were provided as a generous gift by Prof. Varsha Gupta of Government Medical College and Hospital (GMCH), Chandigarh, India. We appreciate Mr. Deepak Bhatt's technical support at the Confocal Microscopy facility. We acknowledge Dr. Kusum Joshi from Chandigarh's Medicos Centre for histopathological evaluations. This research received no specific grant from any funding agency in public, commercial, or not-for-profit sectors.

Author contributions

H.N. and N.C. designed the project. N.C., R.T., and N.M. performed the biological experiments. R.K. and S.J. performed chemical synthesis. A.D. has performed in vitro P.K. Manuscript writing: original draft preparation by N.C; writing—review, editing by N.C. and H.N. All of the authors read and approved the final version of the manuscript.

Competing interests
The authors declare no competing interests.

Ethics approval
This study was carried out in compliance with the recommendations of the Committee for the Purpose of Control and Supervision of Experiments on Animals (CPCSEA). The protocol (IAEC/21/05) was approved by the Institute of Microbial Technology's Institutional Animal Ethics Committee in Chandigarh, India. We have complied with all relevant ethical regulations for animal use. We have used female, BALB/c mice of 5–7 weeks in our experiments. Randomization and blinding were not regarded as necessary for infection animal models. During the histopathology investigation, the observer was unaware of the control and treatment groups.

Additional information
Supplementary information The online version contains supplementary material available at https://doi.org/10.1038/s42003-024-06996-8.

Correspondence and requests for materials should be addressed to Hemraj Nandanwar.

Peer review information *Communications Biology* thanks the anonymous reviewers for their contribution to the peer review of this work. Primary Handling Editors: Cesar de la Fuente and Tobias Goris.